Arabidopsis thaliana 3-mercaptopyruvate sulfurtransferases interact with and are protected by reducing systems

Anna Moseler, Tiphaine Dhalleine, Nicolas Rouhier, Jérémy Couturier

Version of Record: https://www.sciencedirect.com/science/article/pii/S0021925821002027
Manuscript_9361542216271cedd91506ac22ab6b0a

Arabidopsis thaliana 3-mercaptopyruvate sulfurtransferases interact with and are protected by reducing systems

Anna Moseler, Tiphaine Dhalleine, Nicolas Rouhier, Jérémy Couturier

Université de Lorraine, INRAE, IAM, F-54000 Nancy, France

*Corresponding author: Jérémy Couturier

Email: jeremy.couturier@univ-lorraine.fr

Running title: Biochemical characterization of *Arabidopsis* STR1 and *S*TR2

Keywords
Sulfurtransferase, Hydrogen sulfide, Persulfide, Thioredoxin, Glutathione, Cysteine, 3-mercaptopyruvate

ABSTRACT

The formation of a persulfide group (-SSH) on cysteine residues has gained attention as a reversible posttranslational modification contributing to protein regulation or protection. The widely distributed 3-mercaptopyruvate (3-MP) sulfurtransferases (MSTs) are implicated in the generation of persulfidated molecules and H_2S biogenesis through transfer of a sulfane sulfur atom from a suitable donor to an acceptor. Arabidopsis has, two MSTs, named STR1 and STR2, but they are poorly characterized. To learn more about these enzymes, we conducted a series of biochemical experiments including a variety of possible reducing systems. Our kinetic studies, which used a combination of sulfur donors and acceptors revealed that both MSTs use 3-MP efficiently as a sulfur donor while thioredoxins, glutathione and glutaredoxins all served as high affinity sulfane sulfur acceptors. Using the redox-sensitive GFP (roGFP2) as a model acceptor protein, we showed that the persulfide-forming MSTs catalyze roGFP2 oxidation and more generally trans-persulfidation reactions. However, a preferential interaction with the thioredoxin system and glutathione was observed in case of competition between these sulfur acceptors. Moreover, we observed that MSTs are sensitive to overoxidation but are protected from an irreversible inactivation by their persulfide intermediate and subsequent reactivation by thioredoxins or glutathione. This work provides significant insights into Arabidopsis STR1 and STR2 catalytic properties, and more specifically emphasizes the interaction with cellular reducing systems for the generation of H_2S and glutathione persulfide and reactivation of an oxidatively-modified form.

INTRODUCTION

An ever-growing body of evidence indicates that hydrogen sulfide (H_2S) plays a role in cellular signalling as other gaseous molecules such as nitric oxide (NO) and carbon monoxide (CO). Signalling by H_2S is proposed to occur *via* the posttranslational modification (PTM) of critical cysteine residues (RSH) to persulfides (RSSH), called persulfidation, resulting in a cysteine whose thiol group is covalently bound to sulfur (sulfane sulfur) (1). Oxidized thiol species such as sulfenic acids (RSOH), but not reduced thiols, are the direct targets of H_2S reactivity (2–4). Cysteine persulfides have been found in free cysteine, small molecule peptides as well as in proteins (5). Recently, it was demonstrated that prokaryotic and mammalian cysteinyl-tRNA synthetases (CARSs) have a crucial role in the synthesis of cysteine persulfides (Cys-SSH) (6, 7) thus representing one of the numerous pathways contributing to the formation of persulfides.

In plants, H_2S is associated with various physiological functions ranging from responses to abiotic and biotic stresses, plant development (seed germination, root development, leaf senescence), photosynthesis, autophagy to stomatal movement (8). Three distinct enzymatic pathways producing H_2S have been identified. Sulfide is primarily produced in chloroplasts through the action of sulfite reductase during the reductive assimilation of sulfate. It is then incorporated into the amino acid skeleton of O-acetylserine to form cysteine, the biosynthesis of which can occur in the cytosol, plastids and mitochondria (9). Another pathway of H_2S

biogenesis is the conversion of cyanide and cysteine into β-cyanoalanine and H_2S which is catalyzed by the β-cyanoalanine synthase CAS-C1 in mitochondria (8, 10). In the cytosol, the L-cysteine desulfhydrase 1 (DES1) degrades cysteine into H_2S, ammonia and pyruvate (11, 12). Up to now, the links between the H_2S-producing enzymes and the cellular persulfidation state have not been clearly identified in plants. Despite *des1* mutant plants display a reduced sulfide production (30% decrease under steady-state growth conditions) (11) and are affected in several physiological pathways (senescence, autophagy, stomatal closure and immunity), the number of persulfidated proteins in wild-type (WT) and *des1* plants (2015 and 2130, respectively) is similar and with a high overlap of 85% (13). In *des1* mutants, the persulfidation level of only 47 proteins, including protein kinases, protein phosphatases and abscisic acid receptors was decreased underlying a limited role of DES1 in protein persulfidation. Hence, other factors/pathways promoting protein persulfidation in plants remain to be identified.

In mammals, H_2S is generated primarily by three different enzymes: cystathionine beta-synthase (CBS), cystathionine gamma-lyase (CSE), and 3-mercaptopyruvate sulfurtransferase (MST) (14, 15). MSTs belong to the sulfurtransferase (STR) family, which are characterized by the presence of a rhodanese (Rhd) domain (16, 17). Due to the conserved catalytic cysteine present in the rhodanese domain, STRs are implicated in sulfur/persulfide trafficking through their ability to catalyze the transfer of a sulfur atom to nucleophilic acceptors. The MST isoforms are characterized by the presence of two Rhd domains with only the C-terminal one possessing the catalytic cysteine in a characteristic CG[S/T]GVT signature (17). In mammals, MSTs are found in both the cytosol and mitochondria. In rat liver, the specific MST activity is 3-fold higher in mitochondria than in the cytosol (18). In mice, the mitochondrial MST contributes to H_2S metabolism and sulfide signalling by releasing H_2S in the presence of a reductant such as a thioredoxin (TRX) (19, 20). Furthermore, the production of polysulfides H_2S_2 and H_2S_3 by MST has been reported in the absence of reductant (21) whereas Cys-SSH and glutathione persulfide (GSSH) were observed in the presence of physiological concentrations of cysteine and GSH (22). Similar observations were done in *E. coli* with the involvement of the MST ortholog, SseA, in the production of reactive sulfane sulfur and notably GSSH and GSSSH (23). From a physiological point of view, the levels of total persulfidated species in the brain of MST-KO mice are less than 50% of those in the brain of WT mice indicating that mitochondrial MST is indeed an important factor in promoting protein persulfidation (21, 22). The biochemical characterization of human MSTs has confirmed that TRXs are physiological persulfide acceptors contributing to the generation of H_2S and thus TRXs can be considered as regulators of protein persulfide levels in the cells (24).

Whereas good evidence for the function of MSTs in sulfur transfer or H_2S synthesis has been gained in bacteria and vertebrates over the last decade, their function in plants is just being elucidated. Plants possess at least one MST isoform but *Arabidopsis thaliana* has two MSTs, named STR1 and STR2, that are located in mitochondria and cytosol respectively (25, 26). In Arabidopsis, the MSTs are suggested to be multifunctional enzymes involved in cysteine catabolism and sulfide production and possibly in cyanide detoxification as shown *in vitro* (27–30). Regarding the MST role in cysteine degradation in mitochondria, STR1 converts 3-MP, formed by the action of a yet unknown cysteine aminotransferase on cysteine, to pyruvate resulting in the formation of an enzyme-bound persulfide (Fig. S1). It is suggested that STR1 persulfide is then transferred to GSH (28). In accordance with their catalytic mechanism, both Arabidopsis MSTs were isolated as persulfidated proteins from leaf extracts (13). In addition to these functions, an interaction of both MSTs was observed with TRXs through bimolecular fluorescence complementation (BiFC), but no further investigation of the implication of these two systems in H_2S biosynthesis and protein persulfidation has been performed (31).

In this study, we have investigated the kinetics of H_2S biosynthesis and of low-molecular weight persulfide production from 3-MP catalyzed by recombinant Arabidopsis STR1 and STR2 since a fine characterization of their enzymatic properties was not achieved so far. This 3-MP conversion constitutes an efficient H_2S biogenesis system in the presence of the major cellular reductants (TRX, GRX). Other trans-persulfidation reactions, not necessarily releasing H_2S, have been observed with GSH,

Cys or the model acceptor protein roGFP2, suggesting that MSTs could participate in the trafficking of sulfane sulfur and/or in protein oxidation. These results advance our understanding of the roles of these two MSTs. The observed partnership with physiological sulfur acceptors such as TRXs, GRXs and GSH will help mapping sulfur transfer events across interconnected pathways and designing adequate strategies for studying H_2S biogenesis *in planta*.

RESULTS

STR1 and STR2 favour 3-MP as sulfur donor to form persulfides

To analyze the functional facets of Arabidopsis MSTs, the corresponding recombinant proteins were purified after heterologous expression in *E. coli* with a production yield for STR1 of 20 mg and for STR2 of 4 mg of protein from 1 L bacterial culture. Different sulfur-containing compounds were tested as substrates to examine which sulfur donor is preferentially used by STR1 and STR2 *in vitro*. The protein activity was quantified by measuring the DTT-released H_2S through the formation of methylene blue (Fig. S2, 32). The data obtained clearly indicated that 3-MP was the preferred sulfur donor that leads to H_2S production (Fig. 1A). Only a very low activity was observed with thiosulfate as sulfur donor (Fig.1A), although it was shown previously that STR1 possessed a thiosulfate:cyanide sulfurtransferase activity (33). No activity was measured in the presence of cysteine.

The interaction of 3-MP with both STR1 and STR2 was then evaluated using fluorescence measurements. Indeed, some non-plant MSTs exhibit quenched intrinsic fluorescence after forming the intermediate persulfide, due to the location of a tryptophan residue close to the active site (34–36). Similar to *E. coli* SseA or human TUM1, STR1 and STR2 display intrinsic fluorescence with a maximum at 336 nm when excited at 270 nm (Fig. S3A). The fluorescence emission spectra of either Arabidopsis MSTs did not change following the addition of pyruvate but showed a strong decrease after addition of 3-MP (Fig. S3B-D). Thus, we analyzed the fluorescence changes as a function of 3-MP concentration to determine STR dissociation constant for 3-MP. K_d values of 1.3 ± 0.9 µM and 0.7 ± 0.3 µM were obtained for STR1 and STR2 respectively (Fig. 1B). Additionally, STR1 C333S and STR2 C298S variants, in which the catalytically important cysteine residue present in the 6-amino acid CGTGVT signature was substituted for a serine, were generated. The intrinsic fluorescence of both variants also decreased after addition of 3-MP but not as strongly as in STR1 and STR2 indicating that the binding of 3-MP already led to fluorescence quenching, not only persulfide formation (Fig. S3B-D).

Then we examined whether MSTs are able to transfer a persulfide from 3-MP to an acceptor protein. Therefore, we used the redox sensitive green fluorescent protein (roGFP2) as a model acceptor protein to analyze protein trans-persulfidation *in vitro* based on a previous work in which it was observed that roGFP2 can be oxidized through the activity of MSTs using 3-MP as sulfur donor in living cells (37). Considering that 3-MP alone does not trigger roGFP2 oxidation and that the reaction between 3-MP and MSTs leads to the persulfidation of the MST catalytic cysteine, it is likely that this persulfide group is then transferred to one of the Cys of the reduced roGFP2 and that the second Cys of roGFP2 reduces the persulfide, yielding H_2S and an oxidized roGFP2 (Fig. 2A). The resulting intramolecular disulfide bridge of roGFP2 changes the steric arrangement of the beta barrel surface and in turn the optical characteristics of the chromophore enabling a direct read-out of roGFP2 oxidation. Addition of 3-MP to the MST and roGFP2 mix led indeed to an efficient oxidation of roGFP2, whereas no oxidation was observed in the absence of MST or using variants mutated for the conserved active site Cys of the MST (STR1 C333S and STR2 C298S) (Fig. 2B, C). Altogether, these findings indicate that STR1 and STR2 form persulfides on the catalytic cysteine after treatment with 3-MP which is the canonical substrate *in vitro* and are able to transfer the persulfide to an acceptor.

STR1 and STR2 efficiently produce H_2S in the presence of various physiological acceptors

Previously it was suggested that STR1 plays a role in cysteine degradation by transferring a persulfide from 3-MP to GSH (28) and additionally, it was reported through BiFC that STR1 and STR2 interact with the mitochondrial TRXo1 or cytosolic TRXh1, respectively (31). These results prompted us to investigate the interaction of the MSTs with a larger panel of physiologically relevant sulfane

sulfur acceptors, GSH and cysteine, but also TRX or GRX reducing systems and to determine the steady-state kinetic parameters associated with H_2S generation (Table 1). In all cases, a hyperbolic relationship between the rate of reaction and the concentration of acceptor was obtained (Fig. S4A-E). Catalytic efficiencies (k_{cat}/K_m) ranging from 1.3 x 10^6 to 8.7 x 10^6 M^{-1} s^{-1} have been measured in the presence of the TRX or GRX reducing systems for both STR1 and STR2, which are 10 to 100-fold higher than the values obtained with GSH or cysteine (Table 1). The apparent K_m values for the two mitochondrial TRXo1 and TRXo2 as well as the cytosolic TRXh1 were in the low micromolar range ranging from 1.3 to 5.3 µM. Similar apparent K_m values around 3 µM were recently estimated for the human MPST1 and MPST2 with the cytosolic thioredoxin TXN (24). In contrast, the apparent K_m values of STR1 or STR2 for GSH, 200 µM or 350 µM respectively, differ considerably from the value of 28 mM obtained for human MPST2 (38). Interestingly, apparent K_m values of 0.7 to 4.6 µM were measured for GRXs (GRXC1 and C4) using both STRs indicating that MST activity can be also coupled to these reductases. Similar steady-state kinetic parameters were determined for STR1 using TRXo1, GRXC1 or GSH by following the NADPH consumption instead of measuring the methylene blue formation (Fig. S5). Finally, the apparent K_m values for 3-MP were estimated at saturating concentrations of each acceptor using mitochondrial TRXo1 and TRXo2 for STR1 and the cytosolic TRXh1 for STR2 and ranged from 290 to 460 µM (Table 2, Fig. S4F). Altogether, these results show that both Arabidopsis MST isoforms have globally similar kinetic constants for each substrate or reducing system tested. The apparent affinities indicate that all these interactions may be physiologically relevant and point for the first time to a possible role of GRXs. Moreover, GSH may have an important role as an acceptor of persulfides from plant MSTs, unlike human MPST.

The ability of both MSTs to oxidize roGFP2 through trans-persulfidation reactions prompted us to analyze whether reducing systems could prevent or compete with this sulfur transfer reaction. In the presence of 1 to 1000 µM GSH, addition of 3-MP led to a minor increase in oxidation of roGFP2 compared to the degree of oxidation in the absence of GSH indicating that GSH indeed competed with roGFP2 as persulfide acceptor (Fig. 3A-B, Fig. S6). Similar results were obtained when the TRX system replaced GSH. After addition of 3-MP a marginal oxidation of roGFP2 was observed in the presence of the complete TRX reducing system in contrast to controls in which just NADPH or NADPH and NTRB were present (Fig. 3C-D). In the presence of NTRB the oxidation of roGFP2 was nevertheless lower indicating that NTRB can reduce to some extent a persulfidated roGFP2 or STR1. Altogether, these results demonstrate that STR1 and STR2 promote preferentially the persulfidation of TRXs and GSH to generate H_2S or GSSH rather than the persulfidation of roGFP2.

Only the reactive catalytic cysteine of MSTs is indispensable to their STR activity

STR1 and STR2 contain 5 and 4 cysteines respectively. Similar to MSTs from other organisms, the C-terminal Rhd-domain of STR1 and STR2 contains the conserved active site cysteine in a CG[T/S]GVT motif (17). The catalytic efficiency of MSTs should be at least partially governed by the reactivity of the catalytic cysteine, which is dependent on its pK_a. Seeking to assess the pK_a of Cys333 of STR1 and Cys298 of STR2, we used a method relying on H_2O_2 as blocking reagent reacting with thiolates but not thiols. The pH-dependent inactivation of STRs by H_2O_2 was followed by comparing their residual activity in the presence of 3-MP and DTT as reductant, after pre-incubation of the reduced proteins in different buffers ranging from pH 2.0 to 9.0 with or without H_2O_2. From these titration curves, we obtained a pK_a value for STR1 of 3.8 ± 0.1 and for STR2 of 4.0 ± 0.1 (Fig. 4). These results indicate that at physiological pH, the thiolate form will be the dominant, almost only, species existing for the catalytic cysteine of both STRs.

Other cysteines present in plant MSTs are usually not conserved in non-plant MSTs. One is present in the N-terminal domain and the others are present in the C-terminal domain (Fig. 5A). To determine whether and how they contribute to the catalytic mechanism of the respective STR, single Cys-to-Ser variants were generated. For STR2, however, only a variant (C298S) for the conserved catalytic cysteine was analyzed because other variants were expressed as insoluble proteins. Using variants mutated for the conserved active site Cys in both STRs, no H_2S was produced from 3-MP in the presence of

TRXs, which underlines its essential role in the reaction mechanism (Fig. 5B). In contrast, STR1 variants mutated for the non-conserved C152, C295, C305 or C340 produced similar amounts of H_2S in our assay, indicating that these cysteines are not important for 3-MP desulfuration.

To gain more insight into the mechanism of MST-dependent H_2S biogenesis through reduction by cellular reducing systems, we measured the activity of STR1 in the presence of single Cys-to-Ser variants of TRX and GRX active site motifs and compared the amount of released H_2S using the respective reducing system. An important reduction of H_2S release (Fig. 5C) was observed using either a variant of the catalytic (TRXo1 C37S) or of the resolving cysteine (TRXo1 C40S) of TRXo1, indicating that both cysteines of TRX are required for persulfide transfer from STR1 and persulfide reduction (Fig. S7A). The residual activity obtained with TRXo1 C37S and C37S/C40S variants suggests that NTRB reduces to some extent a persulfidated STR1 and the slightly higher activity obtained with TRXo1 C40S that NTRB reduces to some extent a persulfidated TRXo1. Increasing the amount of NTRB in the absence of TRX, however, did not increase STR activity (Fig. S7B). The necessity of both Cys for full activity was also observed with the monocysteinic variants of TRXo2 supporting a dithiol mechanism for the TRX-mediated H_2S release from STRs (Fig. S7A, C). Regarding the TRX system, the reaction mechanism is proposed to occur *via* a ping-pong mechanism in which 3-MP binds to the MST and an enzyme-bound persulfide intermediate is formed (1, 36, 38). Following the release of pyruvate, the persulfide is transferred to the catalytic cysteine of the TRX. In the next step, the resolving cysteine of the TRX active site signature reduces the mixed disulfide, yielding H_2S and an oxidized TRX, which is recycled *via* TRX reductase and NADPH (Fig. S7, 24). Interestingly, analyses of the monocysteinic variants of GRXC1, which also possesses a CxxC active site motif as TRXs, revealed that only the catalytic cysteine (GRXC1 C31) is essential for the release of H_2S. Indeed, mutation of the resolving cysteine (GRXC1 C34) did not influence much the amount of released H_2S compared to the native GRXC1 (Fig. 5D). Similar results with the monocysteinic variants of GRXC1 were obtained using STR2. Hence, the GRX-mediated H_2S release from STRs is based on a monothiol mechanism with GSH serving to recycle the catalytic cysteine even though we cannot exclude a contribution of the second resolving cysteine when present (Fig.S7D-E).

The persulfide intermediate of MSTs protects them from H_2O_2-dependent inactivation

Since *pKa* measurements indicated that the STR1/2 catalytic cysteine is sensitive to H_2O_2 inactivation, we wanted next to assess whether having a catalytic persulfide intermediate could have a protective effect. First, we analyzed the influence of the redox state of STR1 on substrate consumption. Therefore, reduced and persulfidated STR1 treated or not with H_2O_2, were incubated with 3-MP in the absence of reductant and product formation was detected by HPLC. The methylene blue method employed previously for activity measurements was not used due to the requirement of a reductant, which would have interfered with the redox state of the persulfidated protein. Pyruvate was detected in the presence of both reduced and persulfidated STR1 indicating conversion of 3-MP to pyruvate (Fig. S8A, C). In contrast, pre-treatment of the reduced as well as persulfidated STR with H_2O_2 prevented the reaction (Fig. S8B, D). These results demonstrated that persulfidated STR1 was still active in the absence of reductant but its activity is inhibited by H_2O_2 as observed for a reduced STR1.

Recently, Doka and colleagues showed that a persulfidation step prevented the irreversible oxidation of the human serum albumin used as a protein model (39). Therefore, we further compared the sensitivity towards H_2O_2 inhibition of STR1 and STR2 using either reduced or persulfidated forms and the reactivation of their activity by reducing systems. Incubating reduced STR1 and STR2 with an excess of H_2O_2 for 3 min before measuring activity in the presence of the physiological GSH/GR or TRX reducing systems decreased activities up to 60-90% compared to untreated proteins. This loss of activity indicated that a predominantly irreversible oxidation of the catalytic cysteine occurred during the pre-treatment and that none of the reductants could reduce and fully reactivate the MSTs (Fig. 6). In contrast, the activity recovery assays indicated that both persulfidated MSTs treated with H_2O_2 were mostly reversibly oxidized (Fig. 6). The incomplete reactivation compared to the non-

treated persulfidated MSTs is likely due to the incomplete initial persulfidation of STRs. Altogether, these data show that the persulfidation of MSTs protects them against the irreversible oxidation of their catalytic cysteine by H_2O_2 and that both GSH and TRX can reduce RSSH species but also RSSO(n)H species resulting from the oxidation of persulfide groups by H_2O_2 (15).

DISCUSSION

Arabidopsis MSTs share common properties with non-plant orthologs

In the *A. thaliana* genome 21 STRs are annotated, but their specific functions are yet largely unknown (40). The mitochondrial STR1 and cytosolic STR2 are the sole MSTs (17). Accordingly, the *in vitro* activity of STR1 and STR2 was much higher when 3-MP was used as sulfur donor in comparison to thiosulfate (Fig. 1), which is in line with previous results obtained on STR1 (31, 37) and *E. coli* SseA (34) but different from mouse MST for which H_2S-producing activities were the same using 3-MP and thiosulfate (20). Both STR1 and STR2 displayed K_d values for 3-MP close to 1 µM (1.3 ± 0.9 µM and 0.7 ± 0.3 µM, respectively, Fig. 1B) which are in the same range as the K_d value of 5 ± 0.2 µM determined for *E. coli* SseA (34). Despite the presence of several cysteine residues in their primary sequence, only the catalytic cysteine is indispensable for the catalytic activity of STR1 and STR2 (Fig. 4). Accordingly, pK_a values of 3.8 ± 0.1 and of 4.0 ± 0.1, respectively, have been measured for the catalytic cysteine of both STR1 and STR2, values close to the one measured for human MST (5.2 ± 0.1) (36). Also, consistent with the known catalytic mechanism of MSTs, STR1 and STR2 are persulfidated in the presence of 3-MP and were identified in an Arabidopsis persulfidome (13). Using roGFP2 as a model acceptor protein, we confirmed that both STR1 and STR2 were able to catalyze trans-persulfidation (*i.e.,* sulfur transfer from a donor to an acceptor) reaction from 3-MP to a protein acceptor that is not a TRX (Fig. 2). In a similar manner, the yeast MST isoform, TUM1, acts as a sulfur carrier between the cysteine desulfurase Nfs1 and Uba4, another Rhd - containing protein implicated in tRNA thio-modification (42). This sulfur relay system is conserved in human where MST1 interacts with Nfs1 and CNX5 (the human ortholog of Uba4) suggesting a dual function of MST1 both in sulfur transfer for the biosynthesis of molybdenum cofactor (Moco) and tRNA thio-modification in cytosol (35). Up to now, no physiological evidence has confirmed the existence of a similar sulfur relay in plants. Moreover, a role of STR2 in Moco biosynthesis and/or tRNA thiolation appears unlikely since *str2* mutant lines have no phenotype whereas *cnx5* mutants are strongly affected, exhibiting a dwarf phenotype with slightly green and morphologically aberrant leaves (29, 43). From a more general point of view, despite the existence of long lists of possible persulfidated proteins in plants (13) as in other organisms (4, 44), it is yet unknown to which extent MSTs serve as a sulfur relay/trafficking protein participating in protein persulfidation.

Arabidopsis MSTs efficiently produce H_2S through their interaction with TRXs and GRXs

The interaction of mammalian or bacterial MSTs with TRXs was reported to serve for the biogenesis of H_2S (20, 24, 36, 38). In addition, STR1 was reported to interact with the mitochondrial TRXo1 and STR2 with the cytosolic TRXh1 using BiFC studies performed in Arabidopsis protoplasts (31). Our *in vitro* activity assays confirmed these interactions and additionally showed that STR1 also interacts with the mitochondrial TRXo2 (Table 1). All plant MST-TRX couples studied in this work (*i.e.* STR1-TRXo1, STR1-TRXo2 and STR2-TRXh1) catalyzed the formation of H_2S from 3-MP (Table 1, Fig. S4). Kinetic parameters of these reactions including the apparent K_m values for TRX and 3-MP are in the same range as those determined of human MST1 and MST2 orthologs (24, 38). Nevertheless, the catalytic efficiency of both STR1 and STR2 (1×10^6 to 2.8×10^6) is ten to twenty-fold higher than human MSTs ($1.3\text{-}1.4 \times 10^5$) suggesting that plant MSTs are more efficient and/or that TRXs are more efficient physiological sulfur acceptors (Table 1). A preferential interaction of STR1 and STR2 with TRXs was also evident from the inhibition effect of TRXs in the MST-mediated roGFP2 oxidation assay (Fig. 3). Canonical TRXs are characterized by the presence of two cysteine residues in their active site, both of them being indispensable for their activity. Accordingly, a decreased H_2S release was observed in the presence of TRX variants mutated for either cysteines (Fig. 5). Hence, the reaction of STR1 with dithiol TRXs results in

the formation of a persulfide intermediate on the TRX catalytic Cys, which rapidly evolves to generate a disulfide-bridged TRX and to release H_2S. Interestingly, the catalytic efficiency of the reactions in the presence of GRXs is similar to those achieved in the presence of TRXs (Table 1). These results illustrate that GRXs also represent potential partners of MSTs for H_2S biosynthesis. Unlike TRXs, only the catalytic cysteine is required for the GRX activity at least in the presence of GSH (Fig. S7D) (45, 46). Hence, once the catalytic cysteine of GRX is persulfidated, several possibilities exist considering monothiol or dithiol GRXs (Fig. S7E). For dithiol GRXs, the persulfide reduction by the second active cysteine might release H_2S directly without the intervention of GSH. The reduction of the persulfidated GRXs by GSH would lead to the formation of GSSH and possibly to H_2S release upon reaction with a second GSH molecule. The latter pathway applies for monothiol GRXs. From a physiological point of view, no MST-GRX interaction was described so far since studies concentrated mostly on the mitochondrial STR1 and there is no class I GRX in Arabidopsis mitochondria (47–49). However, such an interaction would be relevant for the cytosolic STR2.

In any case, the interaction of the STRs with both reducing systems occurs *via* protein persulfidation and may lead to the production of the signalling molecule H_2S. Given the stable but reversible nature of protein persulfides, a cellular depersulfidation mechanism *via* a depersulfidase should prevent the accumulation of persulfides. For instance, TRX efficiently reduces the persulfidated cysteine in the protein-tyrosine phosphatase 1B (PTP1B), human and bovine serum albumin (HSA and BSA) but also free Cys-SSH (3, 50, 51). Noteworthy, the mammalian selenocysteine (Sec)-thioredoxin reductase exhibits itself polysulfide reducing activity *in vitro* and this is improved by the presence of TRXs (51). In contrast, increased amounts of Arabidopsis NTRB, which does not possess a selenocysteine residue, had no stimulatory effect on STR activity (Fig. S7B). Hence, in the plant system, the interaction of STR1 with TRXs rather than NTR is important. In a similar manner, the mammalian GRX/GSH system efficiently reduces both polysulfides and persulfidated BSA *in vitro* (51). The depletion or deletion of genes encoding thioredoxin reductase or glutathione reductase in animal cells is associated with increased intracellular persulfide levels (3, 39, 51). This underlines the importance of these reducing systems in protein persulfidation mechanisms, notably as a reducing mechanism that can regenerate native forms of Cys residues from persulfide species (51). Whether they act directly in the source by interfering only with persulfide-generating enzymes such as MSTs and/or whether they interact specifically with some persulfidated proteins is an important question. Interestingly, in *S. oleracea* seedlings treated with 100 µM NaHS, gene expression of the TRX reducing system is increased suggesting a role in H_2S producing conditions (52). While TRXs, GSH, and GRXs are clearly important regulators of H_2S production from persulfidated proteins including MSTs, it seems important now to analyze *in vivo*, if deletion of TRXs and/or GRXs leads to increased persulfide levels in plants.

Arabidopsis MSTs generate low molecular weight (LMW) persulfides

Although the catalytic efficiency of the reaction is 100 to 1000-fold lower than values obtained with TRXs or GRXs, the ability of MSTs to release H_2S in the presence of GSH and Cys suggests that LMW persulfides, such as Cys-SSH or GSSH persulfides, are formed. These data are consistent with the proposed role of STR1 in cysteine catabolism which is to produce GSSH as a substrate for ETHE1 (28). Interestingly, the affinity of both Arabidopsis MSTs for GSH (*i.e.*, 200 µM and 350 µM respectively) is much better than the one of human MST ($K_{m,GSH}$ of 28 mM) and thus the catalytic efficiency ($k_{cat}/K_{m,GSH}$) of Arabidopsis MSTs is 5,000 to 20,000-fold higher (Table 1, 23, 24). Considering that GSH concentrations in the cytosol and mitochondria of plant cells are in the mM range (53), the reaction leading to GSSH formation should not be hampered by changes in GSH concentration or oxidation even those occurring during oxidative stress. This should be different in mammals where the MST-dependent GSSH formation should be negligible. Also no reaction of mouse MST with GSH was observed (20), while GSSH concentrations of 35 pmol/mg protein (7 µM) in mouse liver tissue were recently estimated by mass spectrometry (39). This GSSH production is assumed to originate from the enzymatic reaction catalyzed by the mitochondrial sulfide-quinone oxidoreductase (SQR) during H_2S

oxidation (54, 55). The different properties of Arabidopsis MSTs may be related to the absence of SQR in plants whereas it is present in most organisms (56).

Cysteine has been recently proposed to represent a significant sulfur acceptor of human MSTs, leading to the generation of LMW persulfides, despite poor K_m values (3.8 to 4.5 mM) and low reaction rates (1 x 10^2 M^{-1} s^{-1}) (24). Interestingly, STR1 and STR2 display more favourable kinetic parameters, with K_m values of 1.3 to 2.2 mM and a 10-fold higher value of catalytic efficiency (Table 1). This suggests that plant MSTs may represent physiological producers of Cys-SSH in addition to GSSH. The physiological relevance of the LMW persulfide Cys-SSH, at least for mitochondria, was shown by markedly altered mitochondrial morphology in *CARS2* KO human cells or human patients with mutated *CARS*2 (6, 57). The decreased persulfide production affected also mitochondrial biogenesis and bioenergetics. Hence, Cys-SSH is metabolized through the action of the electron transport chain of mitochondria leading to the formation of H_2S.

Reducing systems are also involved in the redox control of Arabidopsis MSTs

Several PTMs of Cys residues such as glutathionylation, disulfide formation, nitrosylation can affect the protein structure and function and play important roles in various biological contexts such as stress conditions or germination (58, 59). Similarly, protein persulfidation reversibly alters enzyme function (60). Under standard growth conditions, at least 5% of the proteome of Arabidopsis leaves undergo persulfidation indicating an important role of this PTM (13). The persulfidation of DES1 and NADPH oxidase RBOHD have been recently related to an increase of both protein activity in relationship with the control of ABA signalling in Arabidopsis guard cells (61). The NaHS-induced persulfidation promotes an increase of the catalytic activity of Arabidopsis glyceraldehyde-3-phosphate dehydrogenase (GAPDH) isoform C1 (GAPC1) and ascorbate peroxidase 1 (APX1) *in vitro* (62). In a similar manner, after NaHS-induced persulfidation, the catalytic activity of an animal GAPDH increases *in vitro* (63). This is consistent with the decrease of GAPDH activity in the liver of a mouse $CSE^{-/-}$ null mutant which contains markedly reduced H_2S levels (63, 64). In contrast, other proteins like papain, a papaya proteinase I, or human tyrosine phosphatase PTP1B are inactivated through persulfide formation of an active site Cys (2, 50). For STR1 and STR2, we did not find an altered activity of persulfidated STR compared to reduced STR (Fig. 6) indicating no regulatory function of the persulfide itself on the MSTs. Already persulfidated STR1 was still able to convert 3-MP into pyruvate (Fig. S8) leading to the formation of a polysulfide. However, after H_2O_2 treatment, the persulfidated STR1 did not catalyze anymore 3-MP conversion into pyruvate. Presence of the GSH/GR or TRX reducing system regenerated a reduced thiol and subsequently the activity (Fig. 6). Thus, in addition to be a catalytic intermediate, the persulfide of MST may exert a protective role in oxidizing conditions. In addition, formation of a polysulfide on MSTs could also serve as a storage of sulfane sulfur. The mitochondrial STR1 was identified as a protein possessing redox-sensitive thiol residue(s) when isolated mitochondria are fed with citrate (59). The identified peptide did not include the active site Cys but C295, which is conserved in land plant orthologs, and C305, which is just present in STR1, indicating that one or both residues exhibit reactivity (17). Although a mutation of these Cys residues did not affect the 3-MP desulfuration activity of STR1 *in vitro* (Fig. 5), a regulatory role *via* the formation of a redox PTM might thus be considered.

Conclusions

The present biochemical study of Arabidopsis STR1 and STR2 indicates that both MSTs use 3-MP as canonical substrate and are able to transfer the persulfide to various acceptors. The formation of the LMW persulfide, GSSH, in the presence of GSH supports a role of STR1 in cysteine degradation as previously reported (28). Furthermore, this work expands the picture, showing that both MSTs can also generate Cys-SSH and can interact with cellular reducing systems for the generation of H_2S (Fig. 7). The interaction between MSTs and TRXs or GRXs suggests that both reducing systems play a role in the regulation of persulfide levels. Nevertheless, further work is necessary to understand how exactly persulfide levels are regulated *in vivo*. The biochemical characterization of the two Arabidopsis MSTs regarding their ability to transfer a persulfide together with the use of roGFP2 as a new tool to analyze MST activity provide scope for future research. Functional characterization of both

MSTs has previously demonstrated that the mitochondrial STR1 contributes the main MST activity (29). Phenotypic analyses revealed that *str1* null mutants show a shrunken seed phenotype with ~87.5% of the embryos arresting at the heart stage whereas the residual 12.5% can develop further and show a normal development of vegetative tissue. In contrast, *str2* null mutants have no identified phenotype (29). However, the double *str1str2* mutant is not viable indicating an essential function of both STRs, which could be a direct contribution to protein persulfidation or the formation of H_2S and/or LMW persulfides.

EXPERIMENTAL PROCEDURES

Materials

3- MP (sodium salt) was purchased from Santa Cruz Biotechnology (Dallas, TX, USA), L-cysteine, thiosulfate, GSH and dithiothreitol were from Sigma-Aldrich (St Louis, MO, USA).

Cloning and site-directed mutagenesis

The sequences coding for the presumed mature forms (*i.e.* devoid of mitochondrial targeting sequences) of *A. thaliana* STR1 (At1g79230.1) and STR2 (At1g16460.2) were cloned into the *Nco*I and *Xho*I restriction sites of pET28a and into the *Nde*I and *Bam*HI restriction sites of pET12a, respectively to obtain untagged versions of STR1 and STR2. The Arabidopsis STR1 was also cloned into the pET28a vector using the STR1 rev2 primer to obtain a C-terminal His-tagged STR1 version. All cysteine residues were individually substituted into serine residues from pET28a-STR1-His or pET12a-STR2 using mutagenic oligonucleotides and the QuikChange site-directed mutagenesis kit (Agilent Technologies). The corresponding variants were named STR1 C152S, C295S, C305S, C333S, C340S and STR2 C117S, C260S, C298S and C305S. All primers used in this study are listed in Supplemental Table 1.

Heterologous expression in E. coli and purification of recombinant proteins

For protein production, the *E. coli* BL21 (DE3) strain was transformed with the recombinant pET12a or pET28a plasmids, the strain expressing also the pSBET helper plasmid (encoding the AGG and AGA codon-recognizing tRNA) in combination with the pET12a plasmid. Cells were grown at 37°C to an OD_{600} of ~0.8 in selective LB medium and high level of protein expression was achieved by addition of isopropyl β-D-thiogalactopyranoside (IPTG) to a final concentration of 100 µM. The cultures were harvested either after 4 h growth at 37°C for expressing STR1 or after 16 h growth at 20°C for expressing STR2. After centrifugation (20 min at 6,380 *g*), the cell pellets were resuspended in about 20 mL of TE NaCl (30 mM Tris-HCl pH 8.0, 1 mM EDTA, 200 mM NaCl) for untagged proteins or in 50 mM Tris-HCl pH 8.0, 300 mM NaCl, 10 mM imidazole for His-tagged proteins and conserved at -20°C. Cell lysis was performed by sonication (3 x 1 min with intervals of 1 min) and the soluble and insoluble fractions were separated by centrifugation for 30 min at 27,216 *g* at 4°C.

For His-tagged proteins, the soluble fraction was loaded on a Ni^{2+} affinity column (Sigma-Aldrich). After extensive washing, proteins were eluted by adding 50 mM Tris-HCl pH 8.0, 300 mM NaCl, 250 mM imidazole. The recombinant proteins were concentrated and dialysed by ultrafiltration under nitrogen pressure (Amicon, YM10 membrane) and stored in a TE buffer supplemented with 50% glycerol at -20°C.

For untagged proteins, the soluble fraction was first precipitated by ammonium sulfate from 0 to 40% and then to 80% of the saturation after a centrifugation step (30 min at 27,216 *g* at 4°C). STR2 and STR1 precipitated mostly between 0 and 40% and between 40 and 80% ammonium sulfate precipitation, respectively. The precipitated fractions were subject to gel filtration chromatography (ACA34) equilibrated with TE NaCl buffer. After dialysis against TE buffer and concentration, the interesting fractions were loaded on a DEAE (diethylaminoethyl) sepharose column equilibrated in TE buffer. All proteins were retained and eluted using a linear 0 to 0.4 M NaCl gradient. The purest fractions as judged by SDS-PAGE gel analysis were pooled and dialysed against TE buffer by ultrafiltration in Amicon cells equipped with a YM10 membrane. Finally, the fractions were concentrated and stored at -20°C in the presence of 50% glycerol in addition to the buffer until further use. Protein concentrations were determined spectrophotometrically in TE buffer using molecular extinction coefficients at 280 nm of 61,670 M^{-1} cm^{-1} for STR1 and its monocysteinic variants and of 64,650 M^{-1} cm^{-1} and 64,525 M^{-1} cm^{-1} for STR2 and its monocysteinic variants, respectively.

Other recombinant proteins used in this work e.g. GRXC1, GRXC4, TRXh1 and TRXh3 from poplar, NADPH-dependent thioredoxin reductase b (NTRB), TRXo1 and TRXo2 from *A. thaliana* as well as roGFP2 have been purified as described previously (45, 65–67). Glutathione reductase from baker's yeast was purchased from Sigma-Aldrich.

Determination of kinetic constants

The STR activity was determined at 25°C in a final volume of 400 µL of 30 mM Tris-HCl pH 8.0 by quantifying the H_2S formed and released by a reductant using the methylene blue method. The reaction mixture contained 250 µM 3-MP and different reductants (DTT, cysteine, GSH system, GSH/GRX and TRX systems). The GSH system was composed of 200 µM NADPH, 0.5 U GR, and 0 to 2 mM GSH whereas the GSH/GRX system contained 200 µM NADPH, 0.5 U GR, 250 µM GSH and 0 to 30 µM GRXC4 or GRXC1. The TRX system was composed of 200 µM NADPH, 200 nM NTRB and 0 to 30 µM TRX. Each reducing system was incubated at 25°C for 10 min prior to adding STR protein and 3-MP. Enzyme and substrate concentrations used are indicated in the legend of figures and tables. The reactions were stopped after 10 min by adding 50 µL of 20 mM N,N-dimethyl-p-phenylenediamine dihydrochloride (DMPD in 7.2 M HCl). The addition of 50 µL of 30 mM $FeCl_3$ (in 1.2 M HCl), followed by a 20 min incubation led to formation of methylene blue, which was then measured at 670 nm. Li_2S (1-100 µM) was used for standard curve calibration to calculate the sulfide (S) released. Activities are expressed as mol S mol^{-1} STR min^{-1}. The apparent K_m values for sulfane sulfur acceptors were determined in the presence of 250 µM 3-MP and the following reductant concentrations: Cys (0 to 5 mM), GSH (0 to 2 mM), GRX and TRX (0 to 30 µM). The apparent K_m value for 3-MP was analyzed in the presence of 0-2 mM 3-MP as well as 30 µM TRXo1, TRXo2 (for STR1) or 10 µM TRXh1 (for STR2), 200 µM NADPH and 200 nM NTRB.

For the NADPH consumption assay, 40 nM STR1 was used in the presence of 500 µM 3-MP in a final volume of 400 µL of 30 mM Tris-HCl pH 8.0. The GSH system was composed of 250 µM NADPH, 0.5 U GR, and 0 to 2 mM GSH whereas the GSH/GRX system contained 250 µM NADPH, 0.5 U GR, 250 µM GSH and 0 to 30 µM GRXC1. The TRX system was composed of 250 µM NADPH, 200 nM NTRB and 0 to 30 µM TRXo1. Oxidation of NADPH was monitored at 340 nm.

Three independent reactions were performed at each reductant concentration and apparent k_{cat} and K_m values were calculated by non-linear regression using the Michaelis-Menten equation.

Fluorescence properties of STRs

The intrinsic fluorescence of STR1 and STR2 and their catalytic variants, alone or with a 100-fold excess of 3-MP or pyruvate, was recorded with a Cary Eclipse spectrofluorometer (Varian) with 2 µM samples in 400 µL of 30 mM Tris-HCl pH 8.0 buffer and an excitation wavelength at 270 nm. Control spectra were run with buffer only for each sample and subtracted from the spectra.

The dissociation constants (K_d) of STRs for 3-MP were determined in the presence of 2 µM reduced STRs and 0 to 200 µM 3-MP at 25°C in a final volume of 30 mM Tris-HCl pH 8.0. The intrinsic fluorescence of the STR protein was immediately measured as described above. Values of fluorescence emission at 337 nm were transformed into percentage of fluorescence decrease by comparison with the value obtained for the reduced protein alone and plotted against the following non-linear regression: Fluorescence decrease =Bmax*[3-MP]/(K_d+[3-MP]) + NS*[3-MP] + Background. Here, Bmax represents the maximum specific binding, NS is the slope of the nonspecific binding line and Background is the fluorescence from the free ligand.

Persulfidation of STRs

Around 5 mg of STRs were reduced using 30 mM DTT in 500 µL of 30 mM Tris-HCl pH 8.0 for 1 h at 25°C. The reduced proteins were then desalted on a G25 column pre-equilibrated with 30 mM Tris-HCl pH 8.0 buffer. Persulfidated STR1 and STR2 were prepared by incubating a reduced protein with a 10-fold excess 3-MP, respectively, for 30 min at 25°C before desalting on G25 column.

Redox state dependence of STR1 activity (HPLC analysis)

The influence of redox state of STR1 on its capacity to transform 3-MP into pyruvate was analyzed by incubating 500 nM STR1 (reduced, reduced treated with 5 mM H_2O_2, persulfidated, or persulfidated and treated with 5 mM H_2O_2)

with 5 mM 3-MP in a final volume of 50 µL of 30 mM Tris-HCl pH 8.0 for 15 min at 25°C. The reactions were stopped by adding 40% ethanol for 10 min before vigorous shaking for 30 s. After centrifugation (10 min at 14,000 rpm), 20 µL of supernatant were injected onto a Synergi Hydro-RP column (150 x 3 mm internal diameter, 4 µm particle size, Phenomenex) equilibrated with 20 mM phosphate buffer pH 4.6 and connected to a Shimadzu Prominence HPLC system. An isocratic elution was used at a flow-rate of 0.5 mL min^{-1} and product detection was monitored at 197 nm. 3-MP and pyruvate standards were separated in similar conditions.

Redox reactivation of oxidized STRs

Pre-reduced and persulfidated STRs (2 µM) were incubated with 2 mM H_2O_2 in 30 mM Tris-HCl pH 8.0 buffer for 3 min at 25°C. Following this pre-incubation step, STR activity was determined by adding 4 µL of the pre-incubation mixture to the 3-MP assay described above with either 1 mM DTT, or GSH system (1 mM GSH, 200 µM NADPH and 0.5 units GR) or TRX system (10 µM TRXo1 for STR1 and TRXh1 for STR2, 200 µM NADPH and 200 nM NTRB) as reductants.

pK_a determination of catalytic cysteine

The acid dissociation constant (pK_a) of the catalytic cysteine of both STR1 and STR2 was determined by measuring the residual activity of reduced forms treated with H_2O_2 at different pH. 2 µM reduced STR was incubated with or without 2 mM H_2O_2 in 100 mM sodium citrate, MES, phosphate or borate buffers ranging from pH 2.0 to 9.0 for 3 min. Following this pre-incubation step, STR activity was determined by adding 4 µL of the pre-incubation mixture to the 3-MP assay described above with DTT as acceptor. The percentages of remaining activity at each pH were determined by comparing the activity of the enzyme incubated with and without H_2O_2 and fitted to the following non-linear regression % activity remaining = Bottom + (Top-Bottom) / (1 + 10^((Log pK_a – pH x HillSlope)).

roGFP2 interaction assay

Interaction of STRs with roGFP2 was analyzed *in vitro* by ratiometric time-course measurements on a fluorescence plate reader (EnSight™ multimode plate reader, PerkinElmer, United States) with excitation at 400 ± 10 nm and 480 ± 10 nm and detection of emitted light at 520 nm with a bandwidth of 10 nm. Ratiometric time-course measurements were carried out with 1 µM reduced roGFP2 and 50 nM STR. For reduction of the protein, roGFP2 was incubated with 10 mM DTT for at least 20 min. The remaining DTT was removed by desalting spin columns according to the manufacturer's manual (Zeba™ Spin Desalting Columns, Thermo Scientific). For interaction analysis with the TRX reducing system, 1 µM TRX, 200 nM NTRB and 200 µM NADPH were added to the reaction mix. The reaction was started by adding 20 µM 3-MP. H_2O_2 and DTT were used at a final concentration of 10 mM to preset roGFP2 to the fully oxidized and fully reduced state, respectively, and to determine maximum and minimum fluorescence ratios of roGFP2 as reference values. A basal background fluorescence of buffer was subtracted from fluorescence reads for all samples. The degree of oxidation (OxD) was determined as described in Aller *et al.*, 2013 (68) according to the equation:

$$OxD_{roGFP2} = \frac{R-R_{red}}{\left(\frac{I_{480ox}}{I_{480red}}\right)(R_{ox}-R)+(R-R_{red})}$$

Here, R denotes the ratio of the fluorescence intensities measured at 400 and 480 nm. R_{red} and R_{ox} represent the fluorescence ratios of fully reduced and fully oxidized roGFP2, respectively. The raw values of I were always corrected by subtracting the respective blank values.

Data availability

All data are presented in the manuscript.

Acknowledgments

This work on plant sulfurtransferases was supported by grant of the ANR-16-CE20-0012 contract. The salary of A.M. was funded by grants of the French National Research Agency (ANR) as part of the "Investissements d'Avenir" program (ANR-11-LABX-0002-01, Lab of Excellence ARBRE) and of the SULPAR (17_GE2_016) GrandEst region contract. A.M. is also recipient of a Feodor Lynen Research Fellowship from the Alexander von Humboldt Foundation.

Author contributions
A.M. and T.D. conceived the research with specific inputs from N.R. and J.C.; A.M. N.R and J.C. designed the experiments and interpreted the data; J.C. conceived the project and wrote the manuscript with A.M. and N.R.; J.C. agrees to serve as the author responsible for contact and ensures communication. All authors read and approved the manuscript.

Conflict of interest
The authors declare that they have no conflicts of interest with the content of this article.

Abbreviations and nomenclature
Sulfurtransferase (STR), 3-mercaptopyruvate sulfurtransferase (MST), thioredoxin (TRX), NADPH thioredoxin reductase (NTR), glutaredoxin (GRX), reduced glutathione (GSH), oxidized glutathione (GSSG), cysteine (Cys), redox-sensitive green fluorescent protein (roGFP), hydrogen sulfide (H_2S), glutathione persulfide (GSSH), posttranslational modification (PTM), cysteinyl-tRNA synthetase (CARS), β-cyanoalanine synthase (CAS), cysteine desulfhydrase 1 (DES1), Wild-type (WT), cystathionine beta-synthase (CBS), cystathionine gamma-lyase (CSE), rhodanese (Rhd), *Escherichia coli* 3-mercaptopyruvate sulfurtransferase (*E. coli* SseA), bimolecular fluorescence complementation (BiFC), dithiothreitol (DTT), thiosulfate sulfurtransferase 1 (TUM1), high performance liquid chromatography (HPLC), low molecular weight (LMW), ethylmalonic encephalopathy protein 1 (ETHE1), sulfide-quinone oxidoreductase (SQR), abscisic acid (ABA), sodium hydrosulfide (NaHS).

REFERENCES

1. Hanaoka, K., Sasakura, K., Suwanai, Y., Toma-Fukai, S., Shimamoto, K., Takano, Y., Shibuya, N., Terai, T., Komatsu, T., Ueno, T., Ogasawara, Y., Tsuchiya, Y., Watanabe, Y., Kimura, H., Wang, C., Uchiyama, M., Kojima, H., Okabe, T., Urano, Y., Shimizu, T., and Nagano, T. (2017) Discovery and mechanistic characterization of selective inhibitors of H2S-producing enzyme: 3-mercaptopyruvate sulfurtransferase (3MST) targeting active-site cysteine persulfide. *Sci. Rep.* **7**, 40227
2. Francoleon, N. E., Carrington, S. J., and Fukuto, J. M. (2011) The reaction of H2S with oxidized thiols: Generation of persulfides and implications to H2S biology. *Arch. Biochem. Biophys.* **516**, 146–153
3. Wedmann, R., Onderka, C., Wei, S., Szijártó, I. A., Miljkovic, J. L., Mitrovic, A., Lange, M., Savitsky, S., Yadav, P. K., Torregrossa, R., Harrer, E. G., Harrer, T., Ishii, I., Gollasch, M., Wood, M. E., Galardon, E., Xian, M., Whiteman, M., Banerjee, R., and Filipovic, M. R. (2016) Improved tag-switch method reveals that thioredoxin acts as depersulfidase and controls the intracellular levels of protein persulfidation. *Chem. Sci.* **7**, 3414—3426
4. Zivanovic, J., Kouroussis, E., Kohl, J. B., Adhikari, B., Bursac, B., Schott-Roux, S., Petrovic, D., Miljkovic, J. L., Thomas-Lopez, D., Jung, Y., Miler, M., Mitchell, S., Milosevic, V., Gomes, J. E., Benhar, M., Gonzalez-Zorn, B., Ivanovic-Burmazovic, I., Torregrossa, R., Mitchell, J. R., Whiteman, M., Schwarz, G., Snyder, S. H., Paul, B. D., Carroll, K. S., and Filipovic, M. R. (2020) Selective persulfide detection reveals evolutionarily conserved antiaging effects of S-sulfhydration. *Cell Metab.* **31**, 1152-1170.e13
5. Millikin, R., Bianco, C. L., White, C., Saund, S. S., Henriquez, S., Sosa, V., Akaike, T., Kumagai, Y., Soeda, S., Toscano, J. P., Lin, J., and Fukuto, J. M. (2016) The chemical biology of protein hydropersulfides: Studies of a possible protective function of biological hydropersulfide generation. *Free Radic. Biol. Med.* **97**, 136–147
6. Akaike, T., Ida, T., Wei, F.-Y., Nishida, M., Kumagai, Y., Alam, M. M., Ihara, H., Sawa, T., Matsunaga, T., Kasamatsu, S., Nishimura, A., Morita, M., Tomizawa, K., Nishimura, A., Watanabe, S., Inaba, K., Shima, H., Tanuma, N., Jung, M., Fujii, S., Watanabe, Y., Ohmuraya, M., Nagy, P., Feelisch, M., Fukuto, J. M., and Motohashi, H. (2017) Cysteinyl-tRNA synthetase governs cysteine polysulfidation and mitochondrial bioenergetics. *Nat. Commun.* **8**, 1–15
7. Fujii, S., Sawa, T., Motohashi, H., and Akaike, T. (2019) Persulfide synthases that are functionally coupled with translation mediate sulfur respiration in mammalian cells. *Br. J. Pharmacol.* **176**, 607–615
8. Gotor, C., García, I., Aroca, Á., Laureano-Marín, A. M., Arenas-Alfonseca, L., Jurado-Flores, A., Moreno, I., and Romero, L. C. (2019) Signaling by hydrogen sulfide and cyanide through post-translational modification. *J. Exp. Bot.* **70**, 4251–4265
9. Takahashi, H., Kopriva, S., Giordano, M., Saito, K., and Hell, R. (2011) Sulfur assimilation in photosynthetic organisms: Molecular functions and regulations of transporters and assimilatory enzymes. *Annu. Rev. Plant Biol.* **62**, 157–184
10. Yamaguchi, Y., Nakamura, T., Kusano, T., and Sano, H. (2000) Three Arabidopsis genes encoding proteins with differential activities for cysteine synthase and β-cyanoalanine synthase. *Plant Cell Physiol.* **41**, 465–476
11. Álvarez, C., Calo, L., Romero, L. C., García, I., and Gotor, C. (2010) An acetylserine(thiol)lyase homolog with cysteine desulfhydrase activity regulates cysteine homeostasis in Arabidopsis. *Plant Physiol.* **152**, 656–669
12. Álvarez, C., García, I., Moreno, I., Pérez-Pérez, M. E., Crespo, J. L., Romero, L. C., and Gotor, C. (2012) Cysteine-generated sulfide in the cytosol negatively regulates autophagy and modulates the transcriptional profile in Arabidopsis. *Plant Cell*. **24**, 4621–4634
13. Aroca, A., Benito, J. M., Gotor, C., and Romero, L. C. (2017) Persulfidation proteome reveals the regulation of protein function by hydrogen sulfide in diverse biological processes in Arabidopsis. *J. Exp. Bot.* **68**, 4915–4927
14. Rose, P., Moore, P. K., and Zhu, Y. Z. (2017) H2S biosynthesis and catabolism: new insights

from molecular studies. *Cell. Mol. Life Sci.* **74**, 1391–1412
15. Filipovic, M. R., Zivanovic, J., Alvarez, B., and Banerjee, R. (2018) Chemical biology of H2S signaling through persulfidation. *Chem. Rev.* **118**, 1253–1337
16. Bordo, D., and Bork, P. (2002) The rhodanese/Cdc25 phosphatase superfamily. *EMBO Rep.* **3**, 741–746
17. Moseler, A., Selles, B., Rouhier, N., and Couturier, J. (2020) Novel insights into the diversity of the sulfurtransferase family in photosynthetic organisms with emphasis on oak. *New Phytol.* **226**, 967–977
18. Nagahara, N., Ito, T., Kitamura, H., and Nishino, T. (1998) Tissue and subcellular distribution of mercaptopyruvate sulfurtransferase in the rat: confocal laser fluorescence and immunoelectron microscopic studies combined with biochemical analysis. *Histochem. Cell Biol.* **110**, 243–250
19. Shibuya, N., Tanaka, M., Yoshida, M., Ogasawara, Y., Togawa, T., Ishii, K., and Kimura, H. (2008) 3-mercaptopyruvate sulfurtransferase produces hydrogen sulfide and bound sulfane sulfur in the brain. *Antioxid. Redox Signal.* **11**, 703–714
20. Mikami, Y., Shibuya, N., Kimura, Y., Nagahara, N., Ogasawara, Y., and Kimura, H. (2011) Thioredoxin and dihydrolipoic acid are required for 3-mercaptopyruvate sulfurtransferase to produce hydrogen sulfide. *Biochem. J.* **439**, 479–485
21. Kimura, Y., Toyofuku, Y., Koike, S., Shibuya, N., Nagahara, N., Lefer, D., Ogasawara, Y., and Kimura, H. (2015) Identification of H2S3 and H2S produced by 3-mercaptopyruvate sulfurtransferase in the brain. *Sci. Rep.* **5**, 14774
22. Kimura, Y., Koike, S., Shibuya, N., Lefer, D., Ogasawara, Y., and Kimura, H. (2017) 3-mercaptopyruvate sulfurtransferase produces potential redox regulators cysteine- and glutathione-persulfide (Cys-SSH and GSSH) together with signaling molecules H2S2, H2S3 and H2S. *Sci. Rep.* **7**, 10459
23. Li, K., Xin, Y., Xuan, G., Zhao, R., Liu, H., Xia, Y., and Xun, L. (2019) Escherichia coli uses separate enzymes to produce H2S and reactive sulfane sulfur from L-cysteine. *Front. Microbiol.* **10**, 298
24. Yadav, P. K., Vitvitsky, V., Carballal, S., Seravalli, J., and Banerjee, R. (2020) Thioredoxin regulates human mercaptopyruvate sulfurtransferase at physiologically relevant concentrations. *J. Biol. Chem.* **295**, 6299–6311
25. Bauer, M., Dietrich, C., Nowak, K., Sierralta, W. D., and Papenbrock, J. (2004) Intracellular localization of Arabidopsis sulfurtransferases. *Plant Physiol.* **135**, 916–926
26. Nakamura, T., Yamaguchi, Y., and Sano, H. (2000) Plant mercaptopyruvate sulfurtransferases. *Eur. J. Biochem.* **267**, 5621–5630
27. Krüßel, L., Junemann, J., Wirtz, M., Birke, H., Thornton, J. D., Browning, L. W., Poschet, G., Hell, R., Balk, J., Braun, H.-P., and Hildebrandt, T. M. (2014) The mitochondrial sulfur dioxygenase ETHYLMALONIC ENCEPHALOPATHY PROTEIN1 is required for amino acid catabolism during carbohydrate starvation and embryo development in Arabidopsis. *Plant Physiol.* **165**, 92–104
28. Höfler, S., Lorenz, C., Busch, T., Brinkkötter, M., Tohge, T., Fernie, A. R., Braun, H.-P., and Hildebrandt, T. M. (2016) Dealing with the sulfur part of cysteine: four enzymatic steps degrade L-cysteine to pyruvate and thiosulfate in Arabidopsis mitochondria. *Physiol. Plant.* **157**, 352–366
29. Mao, G., Wang, R., Guan, Y., Liu, Y., and Zhang, S. (2011) Sulfurtransferases 1 and 2 play essential roles in embryo and seed development in Arabidopsis thaliana. *J. Biol. Chem.* **286**, 7548–7557
30. Papenbrock, J., and Schmidt, A. (2000) Characterization of two sulfurtransferase isozymes from Arabidopsis thaliana. *Eur. J. Biochem.* **267**, 5571–5579
31. Henne, M., König, N., Triulzi, T., Baroni, S., Forlani, F., Scheibe, R., and Papenbrock, J. (2015) Sulfurtransferase and thioredoxin specifically interact as demonstrated by bimolecular fluorescence complementation analysis and biochemical tests. *FEBS Open Bio*. **5**, 832–843
32. Hartle, M. D., and Pluth, M. D. (2016) A practical guide to working with H2S at the interface of chemistry and biology. *Chem. Soc. Rev.* **45**, 6108–6117
33. Burow, M., Kessler, D., and Papenbrock, J. (2002) Enzymatic activity of the Arabidopsis

sulfurtransferase resides in the C-terminal domain but is boosted by the N-terminal domain and the linker peptide in the full- length enzyme. *Biol. Chem.* **383**, 1363–1372
34. Colnaghi, R., Cassinelli, G., Drummond, M., Forlani, F., and Pagani, S. (2001) Properties of the Escherichia coli rhodanese-like protein SseA: contribution of the active-site residue Ser240 to sulfur donor recognition. *FEBS Lett.* **500**, 153–156
35. Fräsdorf, B., Radon, C., and Leimkühler, S. (2014) Characterization and interaction studies of two isoforms of the dual localized 3-mercaptopyruvate sulfurtransferase TUM1 from humans. *J. Biol. Chem.* **289**, 34543–34556
36. Lec, J.-C., Boutserin, S., Mazon, H., Mulliert, G., Boschi-Muller, S., and Talfournier, F. (2018) Unraveling the mechanism of cysteine persulfide formation catalyzed by 3-mercaptopyruvate sulfurtransferases. *ACS Catal.* **8**, 2049–2059
37. Ezeriņa, D., Takano, Y., Hanaoka, K., Urano, Y., and Dick, T. P. (2018) N-acetyl cysteine functions as a fast-acting antioxidant by triggering intracellular H2S and sulfane sulfur production. *Cell Chem. Biol.* **25**, 447–459
38. Yadav, P. K., Yamada, K., Chiku, T., Koutmos, M., and Banerjee, R. (2013) Structure and kinetic analysis of H2S production by human mercaptopyruvate sulfurtransferase. *J. Biol. Chem.* **288**, 20002–20013
39. Dóka, É., Ida, T., Dagnell, M., Abiko, Y., Luong, N. C., Balog, N., Takata, T., Espinosa, B., Nishimura, A., Cheng, Q., Funato, Y., Miki, H., Fukuto, J. M., Prigge, J. R., Schmidt, E. E., Arnér, E. S. J., Kumagai, Y., Akaike, T., and Nagy, P. (2020) Control of protein function through oxidation and reduction of persulfidated states. *Sci. Adv.* **6**, eaax8358
40. Selles, B., Moseler, A., Rouhier, N., and Couturier, J. (2019) Rhodanese domain-containing sulfurtransferases: multifaceted proteins involved in sulfur trafficking in plants. *J. Exp. Bot.* **70**, 4139–4154
41. Papenbrock, J., and Schmidt, A. (2000) Characterization of a sulfurtransferase from Arabidopsis thaliana. *Eur. J. Biochem.* **267**, 145–154
42. Noma, A., Sakaguchi, Y., and Suzuki, T. (2009) Mechanistic characterization of the sulfur-relay system for eukaryotic 2-thiouridine biogenesis at tRNA wobble positions. *Nucleic Acids Res.* **37**, 1335–1352
43. Nakai, Y., Harada, A., Hashiguchi, Y., Nakai, M., and Hayashi, H. (2012) Arabidopsis molybdopterin biosynthesis protein Cnx5 collaborates with the ubiquitin-like protein Urm11 in the thio-modification of tRNA. *J. Biol. Chem.* **287**, 30874–30884
44. Longen, S., Richter, F., Köhler, Y., Wittig, I., Beck, K.-F., and Pfeilschifter, J. (2016) Quantitative persulfide site identification (qPerS-SID) reveals protein targets of H2S releasing donors in mammalian cells. *Sci. Rep.* **6**, 29808
45. Couturier, J., Jacquot, J.-P., and Rouhier, N. (2013) Toward a refined classification of class I dithiol glutaredoxins from poplar: biochemical basis for the definition of two subclasses. *Front. Plant Sci.* **4**, 1–14
46. Zimmermann, J., Oestreicher, J., Hess, S., Herrmann, J. M., Deponte, M., and Morgan, B. (2020) One cysteine is enough: A monothiol Grx can functionally replace all cytosolic Trx and dithiol Grx. *Redox Biol.* **36**, 101598
47. Rouhier, N., Couturier, J., and Jacquot, J.-P. (2006) Genome-wide analysis of plant glutaredoxin systems. *J. Exp. Bot.* **57**, 1685–1696
48. Couturier, J., Jacquot, J.-P., and Rouhier, N. (2009) Evolution and diversity of glutaredoxins in photosynthetic organisms. *Cell. Mol. Life Sci.* **66**, 2539–2557
49. Ströher, E., Grassl, J., Carrie, C., Fenske, R., Whelan, J., and Millar, A. H. (2016) Glutaredoxin S15 is involved in Fe-S cluster transfer in mitochondria influencing lipoic acid-dependent enzymes, plant growth, and arsenic tolerance in Arabidopsis. *Plant Physiol.* **170**, 1284–1299
50. Krishnan, N., Fu, C., Pappin, D. J., and Tonks, N. K. (2011) H2S-induced sulfhydration of the phosphatase PTP1B and its role in the endoplasmic reticulum stress response. *Sci. Signal.* **4**, ra86
51. Dóka, É., Pader, I., Bíró, A., Johansson, K., Cheng, Q., Ballagó, K., Prigge, J. R., Pastor-Flores, D., Dick, T. P., Schmidt, E. E., Arnér, E. S. J., and Nagy, P. (2016) A novel persulfide detection method reveals protein persulfide- and polysulfide-reducing functions of thioredoxin

and glutathione systems. *Sci. Adv.* **2**, e1500968
52. Chen, J., Wu, F.-H., Wang, W.-H., Zheng, C.-J., Lin, G.-H., Dong, X.-J., He, J.-X., Pei, Z.-M., and Zheng, H.-L. (2011) Hydrogen sulphide enhances photosynthesis through promoting chloroplast biogenesis, photosynthetic enzyme expression, and thiol redox modification in Spinacia oleracea seedlings. *J. Exp. Bot.* **62**, 4481–4493
53. Fricker, M. D., May, M., Meyer, A. J., Sheard, N., and White, N. S. (2000) Measurement of glutathione levels in intact roots of Arabidopsis. *J. Microsc.* **198**, 162–173
54. Libiad, M., Yadav, P. K., Vitvitsky, V., Martinov, M., and Banerjee, R. (2014) Organization of the human mitochondrial hydrogen sulfide oxidation pathway. *J. Biol. Chem.* **289**, 30901–30910
55. Zuhra, K., Tomé, C. S., Masi, L., Giardina, G., Paulini, G., Malagrinò, F., Forte, E., Vicente, J. B., and Giuffrè, A. (2019) N-acetylcysteine serves as substrate of 3-mercaptopyruvate sulfurtransferase and stimulates sulfide metabolism in colon cancer cells. *Cells*. **8**, 828
56. Theissen, U., Hoffmeister, M., Grieshaber, M., and Martin, W. (2003) Single eubacterial origin of eukaryotic sulfide:quinone oxidoreductase, a mitochondrial enzyme conserved from the early evolution of eukaryotes during anoxic and sulfidic times. *Mol. Biol. Evol.* **20**, 1564–1574
57. Coughlin, C. R., Scharer, G. H., Friederich, M. W., Yu, H.-C., Geiger, E. A., Creadon-Swindell, G., Collins, A. E., Vanlander, A. V, Coster, R. Van, Powell, C. A., Swanson, M. A., Minczuk, M., Van Hove, J. L. K., and Shaikh, T. H. (2015) Mutations in the mitochondrial cysteinyl-tRNA synthase gene, CARS2 lead to a severe epileptic encephalopathy and complex movement disorder. *J. Med. Genet.* **52**, 532–540
58. Couturier, J., Chibani, K., Jacquot, J.-P., and Rouhier, N. (2013) Cysteine-based redox regulation and signaling in plants. *Front. Plant Sci.* **4**, 1–7
59. Nietzel, T., Mostertz, J., Ruberti, C., Wagner, S., Moseler, A., Fuchs, P., Müller-Schüssele, S. J., Benamar, A., Poschet, G., Büttner, M., Née, G., Møller, I. M., Lillig, C. H., Macherel, D., Finkemeier, I., Wirtz, M., Hell, R., Meyer, A. J., Hochgräfe, F., and Schwarzländer, M. (2020) Redox-mediated kick-start of mitochondrial energy metabolism drives resource-efficient seed germination. *Proc. Natl. Acad. Sci.* **117**, 741–751
60. Bailey, T. S., and Pluth, M. D. (2015) Reactions of isolated persulfides provide insights into the interplay between H2S and persulfide reactivity. *Free Radic. Biol. Med.* **89**, 662–667
61. Shen, J., Zhang, J., Zhou, M., Zhou, H., Cui, B., Gotor, C., Romero, L. C., Fu, L., Yang, J., Foyer, C. H., Pan, Q., Shen, W., and Xie, Y. (2020) Persulfidation-based modification of cysteine desulfhydrase and the NADPH oxidase RBOHD controls guard cell abscisic acid signaling. *Plant Cell*. **32**, 1000–1017
62. Aroca, Á., Serna, A., Gotor, C., and Romero, L. C. (2015) S-Sulfhydration: A cysteine posttranslational modification in plant systems. *Plant Physiol.* **168**, 334–342
63. Mustafa, A. K., Gadalla, M. M., Sen, N., Kim, S., Mu, W., Gazi, S. K., Barrow, R. K., Yang, G., Wang, R., and Snyder, S. H. (2009) H2S signals through protein S-sulfhydration. *Sci. Signal.* **2**, ra72
64. Yang, G., Wu, L., Jiang, B., Yang, W., Qi, J., Cao, K., Meng, Q., Mustafa, A. K., Mu, W., Zhang, S., Snyder, S. H., and Wang, R. (2008) H2S as a physiologic vasorelaxant: Hypertension in mice with deletion of cystathionine γ-lyase. *Science (80-.).* **322**, 587–590
65. Behm, M., and Jacquot, J.-P. (2000) Isolation and characterization of thioredoxin h from poplar xylem. *Plant Physiol. Biochem.* **38**, 363–369
66. Meyer, A. J., Brach, T., Marty, L., Kreye, S., Rouhier, N., Jacquot, J.-P., and Hell, R. (2007) Redox-sensitive GFP in Arabidopsis thaliana is a quantitative biosensor for the redox potential of the cellular glutathione redox buffer. *Plant J.* **52**, 973–986
67. Zannini, F., Roret, T., Przybyla-Toscano, J., Dhalleine, T., Rouhier, N., and Couturier, J. (2018) Mitochondrial Arabidopsis thaliana TRXo isoforms bind an iron–sulfur cluster and reduce NFU proteins in vitro. *Antioxidants*. http://dx.doi.org/10.3390/antiox7100142
68. Aller, I., Rouhier, N., and Meyer, A. (2013) Development of roGFP2-derived redox probes for measurement of the glutathione redox potential in the cytosol of severely glutathione-deficient rml1 seedlings. *Front. Plant Sci.* **4**, 1–12

Table 1. Kinetic parameters of 3-MP sulfurtransferase activity of Arabidopsis STR1 and STR2 using distinct sulfur acceptors.

	STR1			STR2		
	K_m (μM)	k_{cat} (s^{-1})	k_{cat} / K_m (M^{-1} s^{-1})	K_m (μM)	k_{cat} (s^{-1})	k_{cat} / K_m (M^{-1} s^{-1})
TRXo1	5.3 ± 1.0	6.8	1.3 x 10^6	*na*	*na*	*na*
TRXo2	1.3 ± 0.2	3.6	2.8 x 10^6	*na*	*na*	*na*
TRXh1	*na*	*na*	*na*	1.4 ± 0.2	1.4	1.0 x 10^6
GRXC4	1.1 ± 0.1	4.6	4.2 x 10^6	4.6 ± 0.6	2.4	5.2 x 10^5
GRXC1	0.7 ± 0.1	6.1	8.7 x 10^6	1.4 ± 0.29	3.1	2.2 x 10^6
GSH	200 ± 20	5.3	2.7 x 10^4	350 ± 10	2.3	6.6 x 10^3
Cysteine	2200 ± 400	3.9	1.7 x 10^3	1300 ± 70	1.5	1.2 x 10^3

Steady-state kinetic parameters were determined by varying the acceptor concentration at a saturating concentration of 3-MP. *na* = not analyzed, (n = 3; means ± SD).

Table 2: Kinetic parameters of sulfurtransferase activity of Arabidopsis STR1 and STR2 for 3-MP.

	STR1			STR2		
	K_m (μM)	k_{cat} (s^{-1})	k_{cat} / K_m (M^{-1} s^{-1})	K_m (μM)	k_{cat} (s^{-1})	k_{cat} / K_m (M^{-1} s^{-1})
TRXo1	286 ± 5	13.5	4.7 x 10^4	*na*	*na*	*na*
TRXo2	456 ± 24	9.7	2.1 x 10^4	*na*	*na*	*na*
TRXh1	*na*	*na*	*na*	377 ± 15	9.7	2.5 x 10^4

Steady-state kinetic parameters were determined by varying the 3-MP concentration at a saturating concentration of acceptors. *na* = not analyzed, (n = 3; means ± SD).

FIGURE LEGENDS

Figure 1. Substrate specificity of STR1 and STR2.
The substrate specificity (A) of STR1 and STR2 towards 3-MP, thiosulfate and cysteine was evaluated by determining STR activity in the presence of 250 µM sulfur donor and 1 mM DTT. Activity is expressed as mole of sulfide produced by mole enzyme per minute (n = 3; means ± SD). The binding affinity (B) of STR1 and STR2 towards 3-MP was measured in the presence of increasing concentrations of 3-MP analyzing the protein intrinsic fluorescence. The decrease of fluorescence emission at 337 nm was plotted against 3-MP concentration to determine the K_d value. (n = 3; means ± SD).

Figure 2. STR1 and STR2 oxidize roGFP2 through trans-persulfidation reactions.
Suggested reaction mechanism of MST-mediated persulfidation and oxidation of roGFP2 (A). In the first step, the sulfur atom is transferred from 3-MP to the MST, resulting in a cysteine persulfide intermediate in the active site. In the second step, the sulfane sulfur might be transferred to roGFP2 and H_2S liberated resulting in an oxidized roGFP2. The importance of the catalytic cysteine of STR1 (B) and STR2 (C) for the persulfidation and subsequent oxidation of roGFP2 was determined in the presence of 1 µM reduced roGFP2 and 50 nM STR or roGFP2 alone. The arrow indicates the time point of 20 µM 3-MP addition (n = 3).

Figure 3. Both TRX and GSH systems prevent the MST-dependent oxidation of roGFP2.
The impact of each reducing system was determined by using 1 µM reduced roGFP2 in the presence of 50 nM STR1 (A) or STR2 (B) and different amounts of GSH (0-1 mM GSH) or 200 µM NADPH, NADPH/ 200 nM NTRB or NADPH/NTRB/ 1 µM TRXo1 for STR1 (C) and 200 µM NADPH, NADPH/ 200 nM NTRB or NADPH/NTRB/ 1 µM TRXh1 for STR2 (D). The fluorescence of roGFP2 was followed over time and the arrow indicates the time point of 20 µM 3-MP addition (n = 3).

Figure 4. The catalytic cysteines of STR1 and STR2 have low pK_a.
Reduced STRs were incubated with or without 2 mM H_2O_2 in different buffers ranging from pH 2.0 to 9.0 prior to measurement of their activity by using the methylene blue assay. The percentages of remaining activity at each pH were determined by comparing the activity of the enzyme incubated with and without H_2O_2. (n = 3; means ± SD).

Figure 5. Involvement of MST cysteines in 3-MP conversion and interaction with cellular reducing systems.
A. Amino acid sequence alignment of MSTs. Shown are the two Rhd domains with the inactive domain in green and the active domain in blue. The catalytic cysteine of the active site motif is indicated by a red square and other cysteines found in Arabidopsis MSTs by an orange square. The sequence alignment was performed with MUSCLE. Sequences used are: *Ec*SseA (NP_417016), *Sc*TUM1 (NP_014894), *Hs*MST1 (NP_066949), *Zm*MST1 (GRMZM2G029262), *Zm*MST2 (GRMZM2G168888), *Os*MST1 (Os12g41500), *Os*MST2 (Os02g07044), *At*STR1 (AT1G79230), *At*STR2 (AT1G16460).
B. The importance of each cysteine residue of STR1 or STR2 was evaluated by determining the STR activity of the respective monocysteinic variants in the presence of 250 µM 3-MP, 200 µM NADPH, 200 nM NTRB and 30 µM TRXo1 (for STR1) or 10 µM TRXh1 (for STR2), (n = 3; means ± SD).
C. The importance of the catalytic and resolving cysteines of TRXo1 for the activity of STR1 was determined in the presence of 250 µM 3-MP, 10 nM STR1 as well as 25 µM TRXo1 and 200 µM NADPH, 200 nM NTRB (n = 3; means ± SD).
D. The importance of the catalytic and resolving cysteines of GRXC1 for the activity of STR1 was determined in the presence of 250 µM 3-MP, 10 nM STR1 as well as 25 µM GRXC1 and 250 µM NADPH, 250 µM GSH and 0.5 U GR. GSH-dependent activity was subtracted to analyze the additional effect of GRX (n = 3; means ± SD).

Figure 6. Reduced but not persulfidated MSTs are irreversibly inactivated by H_2O_2.

After pre-incubation of 2 µM STR with 2 mM H_2O_2 for 3 min at 25°C, the STR activity was measured with 20 nM STR in the presence of 250 µM 3-MP and GSH/GR system (1 mM GSH, 250 µM NADPH and 0.5 U GR) (A) or TRX system (10 µM TRX (TRXo1 for STR1 and TRXh1 for STR2), 200 µM NADPH and 200 nM NTRB) (B). The values are expressed as percentages of the activity of reduced STRs (STR SH = 100%) (n = 3; means ± SD).

Figure 7. Redox control of the activity of MSTs in Arabidopsis.
MSTs (STR1 and STR2) preferentially use 3-MP as sulfur donor (1). They are implicated in H_2S biogenesis by interacting with TRX or GRX systems (2). By interacting with GSH and cysteine (3), both MSTs might be important for the formation of glutathione persulfide (GSSH) and cysteine persulfide (Cys-SSH). Finally, the oxidation of both reduced (4) and persulfidated catalytic cysteine (5) by H_2O_2 inhibits protein activity but the latter is reversed by the TRX and GSH/GR reducing systems (6).

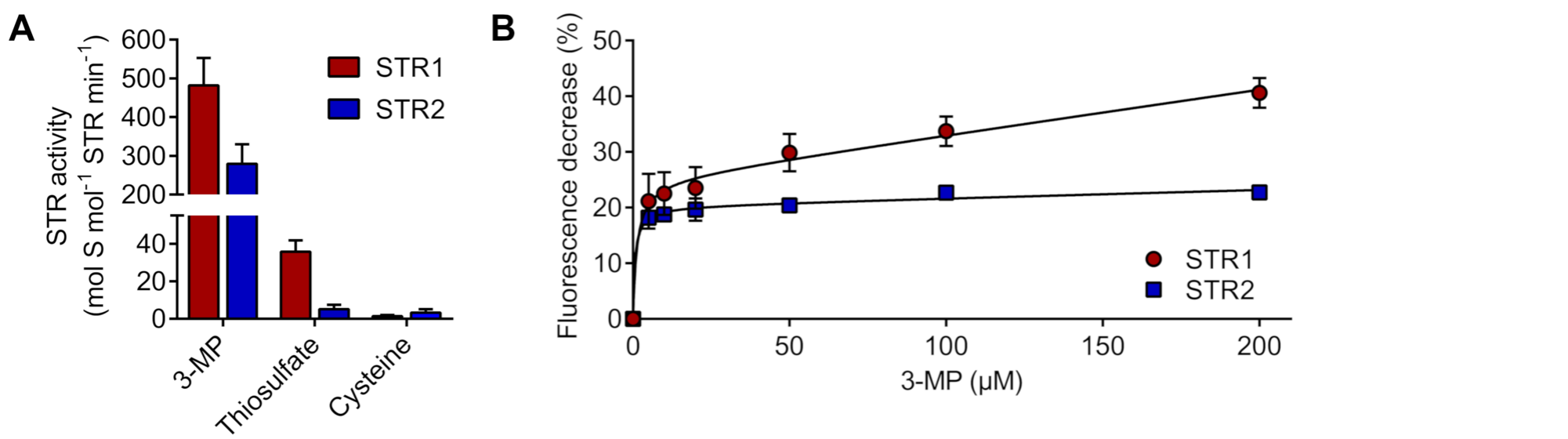
A
STR activity
(mol S mol-1 STR min-1)
600
500
400
300
200
40
20
0
STR1
STR2
3-MP
Thiosulfate
Cysteine
B
Fluorescence decrease (%)
50
40
30
20
10
0
0
50
100
150
200
3-MP (μM)
STR1
STR2

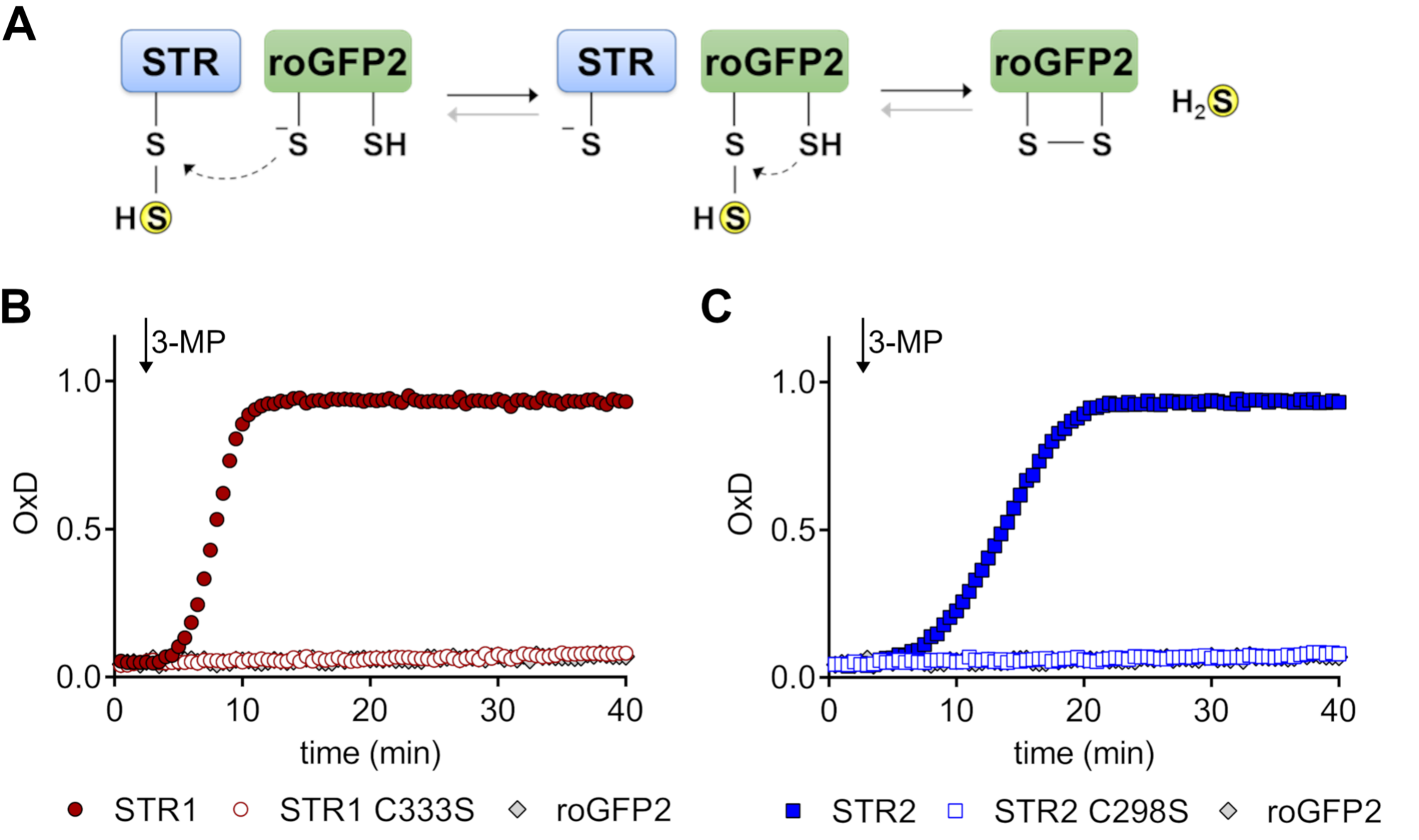
A
STR
roGFP2
STR
roGFP2
roGFP2
H2S
B
3-MP
OxD
time (min)
STR1
STR1 C333S
roGFP2
C
3-MP
OxD
time (min)
STR2
STR2 C298S
roGFP2

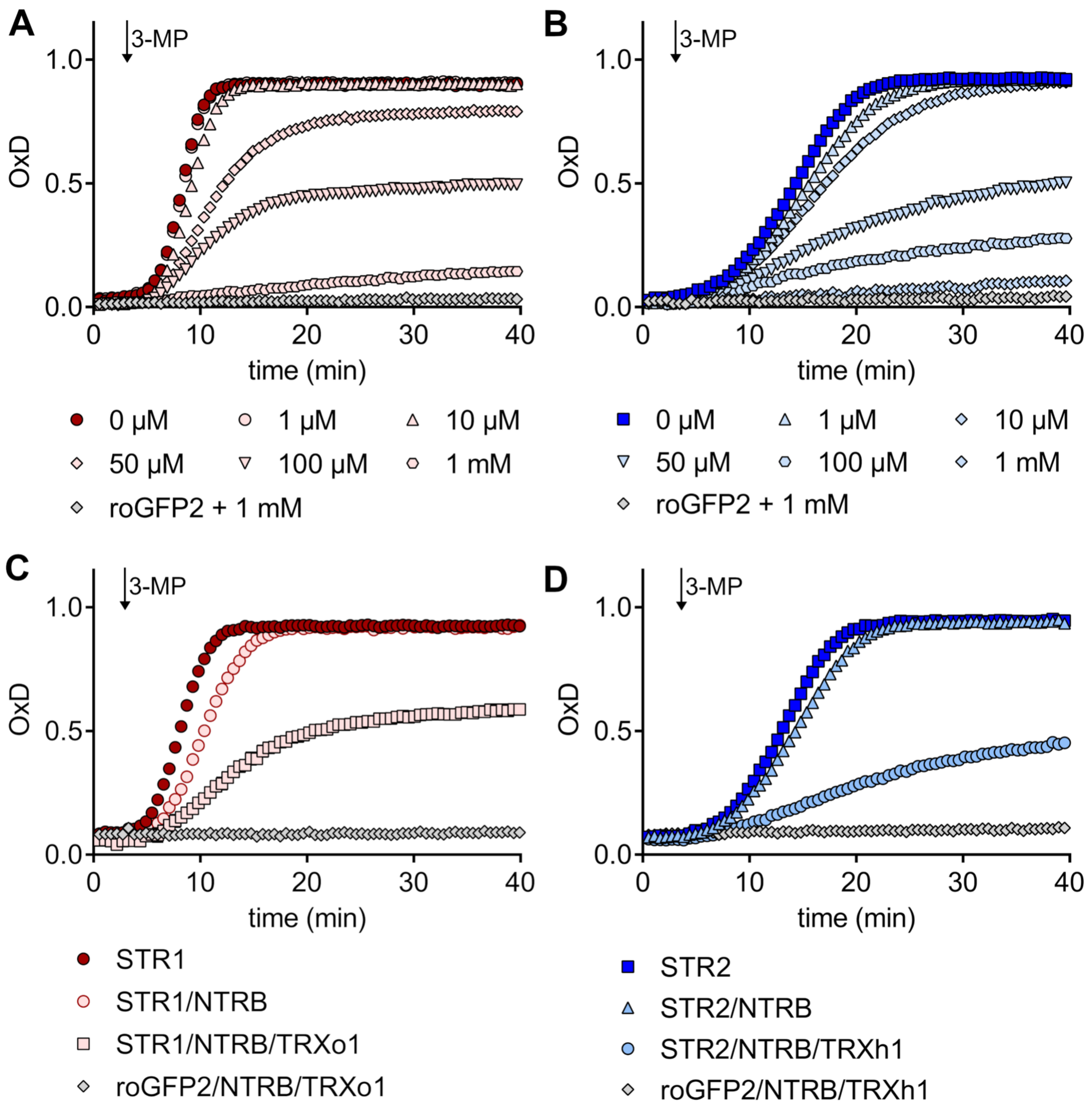
A
3-MP
1.0
0.5
0.0
OxD
0
10
20
30
40
time (min)
0 µM
1 µM
10 µM
50 µM
100 µM
1 mM
roGFP2 + 1 mM
B
3-MP
1.0
0.5
0.0
OxD
0
10
20
30
40
time (min)
0 µM
1 µM
10 µM
50 µM
100 µM
1 mM
roGFP2 + 1 mM
C
3-MP
1.0
0.5
0.0
OxD
0
10
20
30
40
time (min)
STR1
STR1/NTRB
STR1/NTRB/TRXo1
roGFP2/NTRB/TRXo1
D
3-MP
1.0
0.5
0.0
OxD
0
10
20
30
40
time (min)
STR2
STR2/NTRB
STR2/NTRB/TRXh1
roGFP2/NTRB/TRXh1

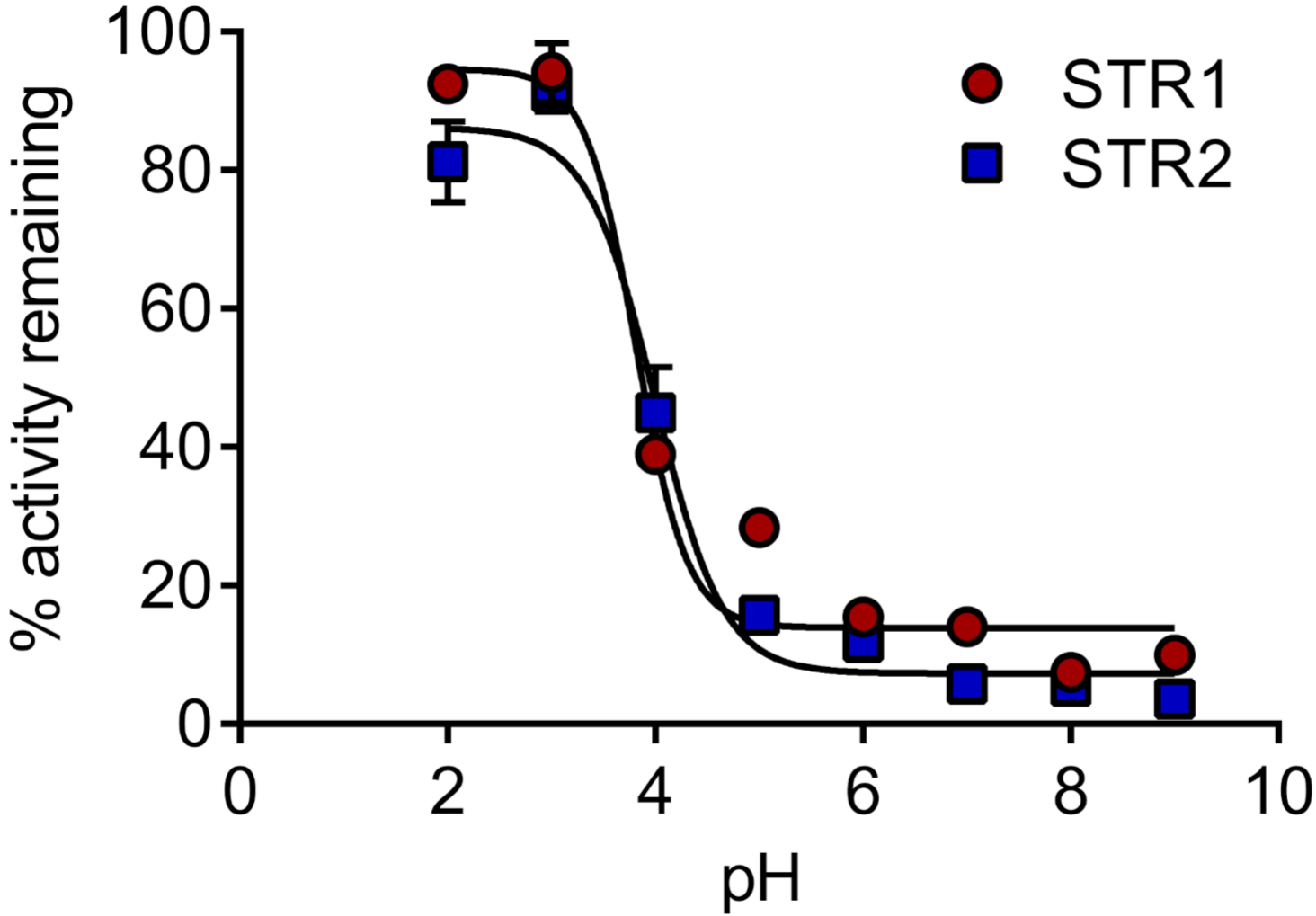
100
80
60
40
20
0
% activity remaining
0
2
4
6
8
10
pH
STR1
STR2

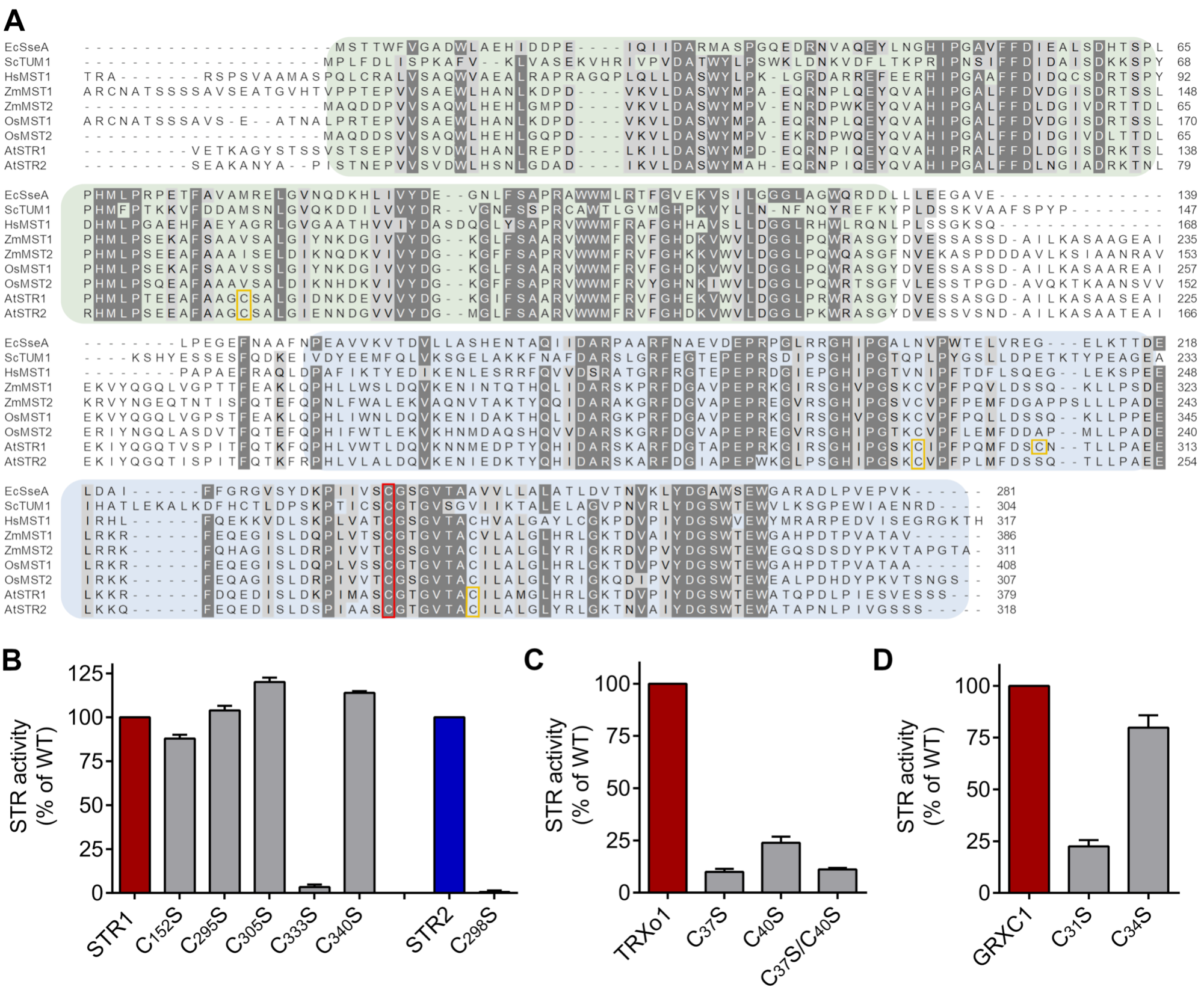
A
EcSseA
ScTUM1
HsMST1
ZmMST1
ZmMST2
OsMST1
OsMST2
AtSTR1
AtSTR2
B
STR activity (% of WT)
125
100
75
50
25
0
STR1
C152S
C295S
C305S
C333S
C340S
STR2
C298S
C
STR activity (% of WT)
100
75
50
25
0
TRXo1
C37S
C40S
C37S/C40S
D
STR activity (% of WT)
100
75
50
25
0
GRXC1
C31S
C34S

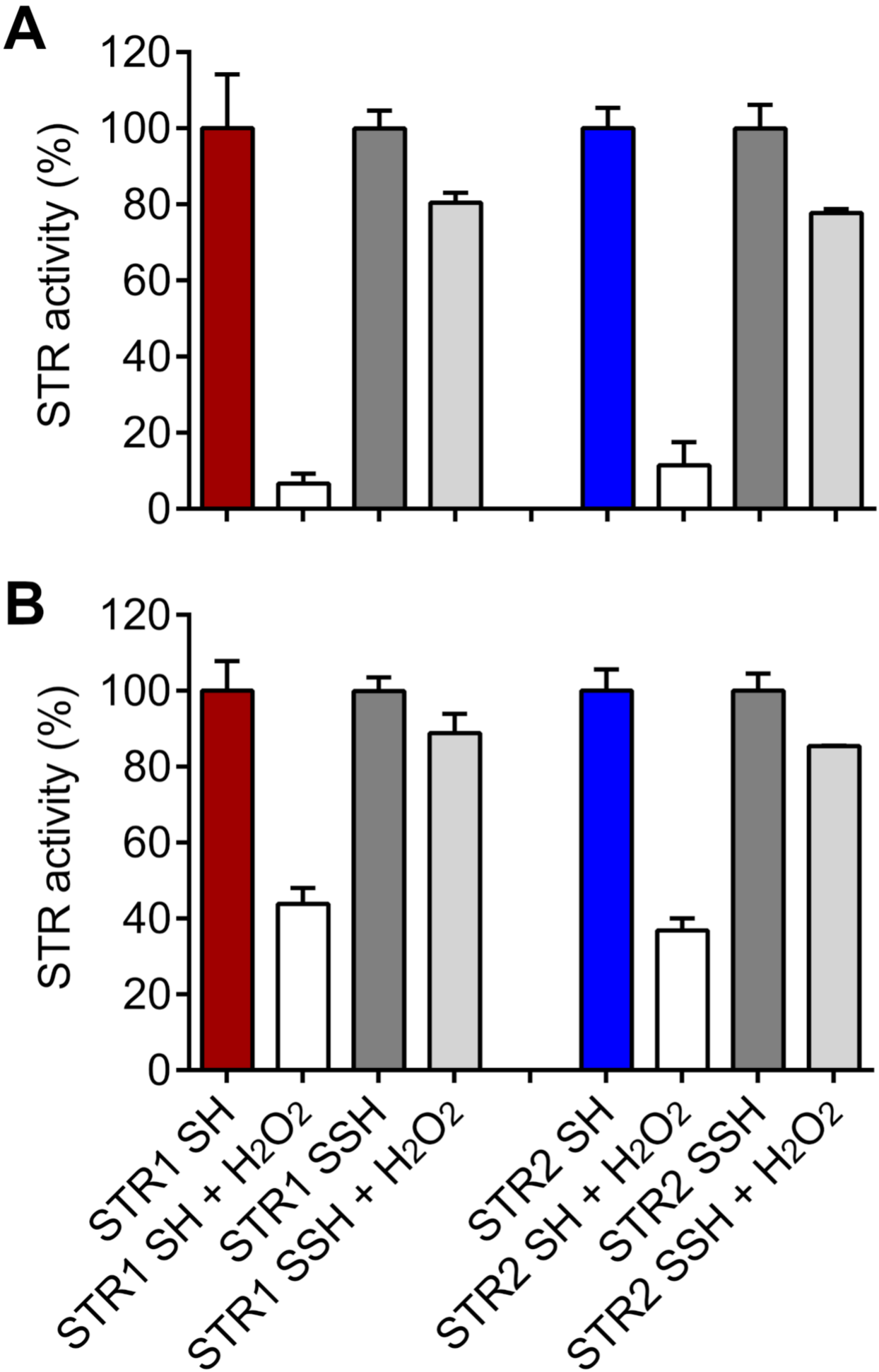
A
STR activity (%)
120
100
80
60
40
20
0
B
STR activity (%)
120
100
80
60
40
20
0
STR1 SH
STR1 SH + H2O2
STR1 SSH
STR1 SSH + H2O2
STR2 SH
STR2 SH + H2O2
STR2 SSH
STR2 SSH + H2O2

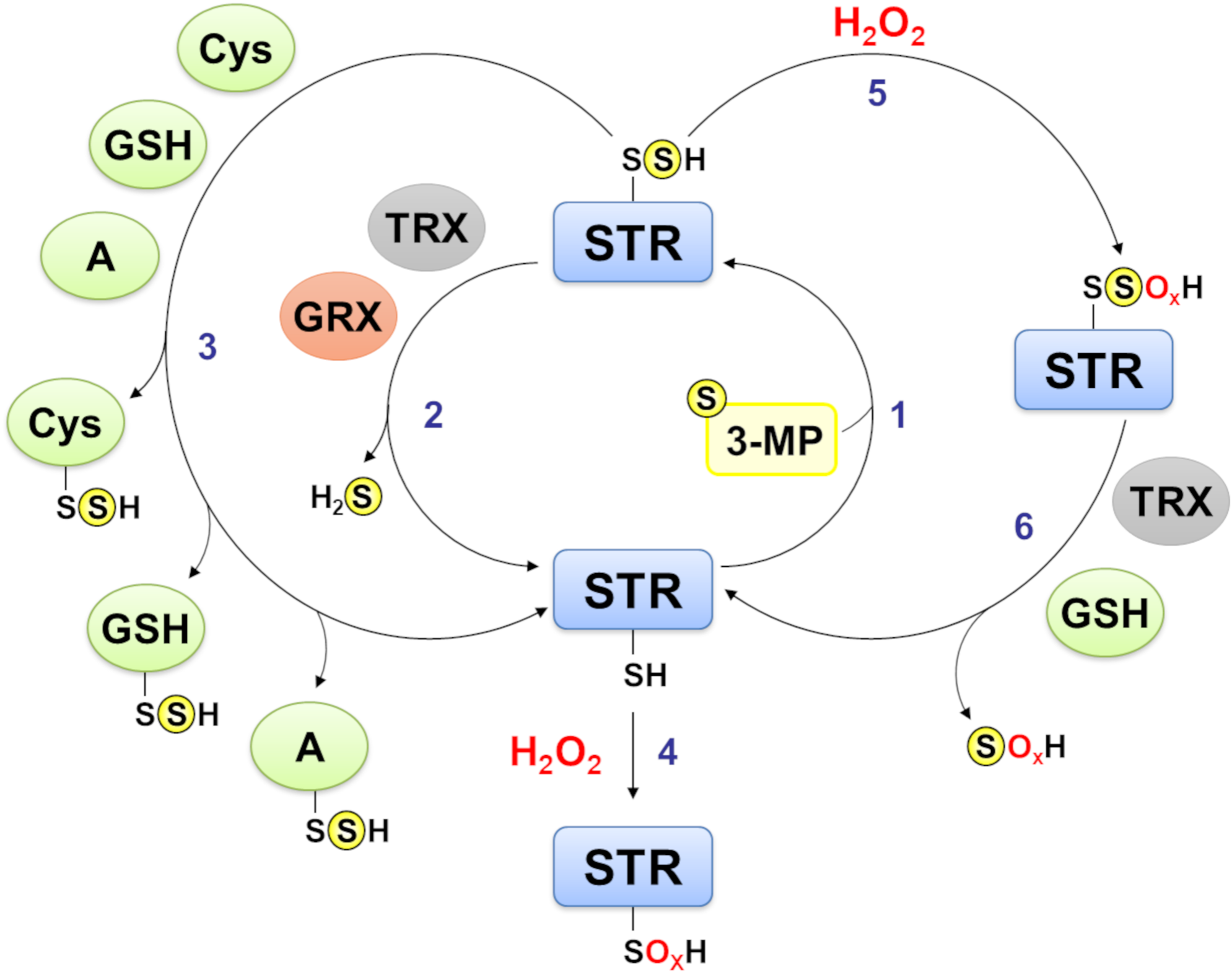
Cys
GSH
A
TRX
GRX
STR
H_2O_2
5
S S H
S S O_xH
STR
3
2
1
S
3-MP
Cys
S S H
H_2S
TRX
6
STR
GSH
GSH
S S H
A
S S H
SH
H_2O_2
4
S O_xH
STR
S O_XH